Confinement Effect of Metal Railing Narrow Baseplates on Adhesive Anchor Breakout Resistance

Final Report
Contract No. BDV28 TWO 977-06
August 2019

Prepared by:

Nakin Suksawang, Ph.D., P.E.
Principal Investigator
Florida Institute of Technology
150 W. University Blvd
Melbourne, FL 32901

For FDOT Project Manager:

Steven Nolan, P.E.
Senior Structures Design Engineer
State Structures Design Office
605 Suwannee Street
Tallahassee, FL 32399-0450

DISCLAIMER PAGE

The opinions, findings, and conclusions expressed in this publication are those of the authors and not necessarily those of the State of Florida Department of Transportation.

APPROXIMATE CONVERSIONS TO SI UNITS

SYMBOL	WHEN YOU KNOW	MULTIPLY BY	TO FIND	SYMBOL
LENGTH				
in	inches	25.4	millimeters	mm
ft	feet	0.305	meters	m
yd	yards	0.914	meters	m
mi	miles	1.61	kilometers	km
AREA				
in^2	squareinches	645.2	square millimeters	mm^2
ft^2	squarefeet	0.093	square meters	m^2
yd^2	square yard	0.836	square meters	m^2
ac	acres	0.405	hectares	ha
mi^2	square miles	2.59	square kilometers	km^2
VOLUME				
fl oz	fluid ounces	29.57	milliliters	mL
gal	gallons	3.785	liters	L
ft^3	cubic feet	0.028	cubic meters	m^3
yd^3	cubic yards	0.765	cubic meters	m^3
NOTE: volumes greater than 1000 L shall be shown in m^3				
MASS				
oz	ounces	28.35	grams	g
lb	pounds	0.454	kilograms	kg
T	short tons (2000 lb)	0.907	megagrams (or "metric ton")	Mg (or "t")
TEMPERATURE (exact degrees)				
°F	Fahrenheit	5 (F-32)/9 or (F-32)/1.8	Celsius	°C
ILLUMINATION				
fc	foot-candles	10.76	lux	lx
fl	foot-Lamberts	3.426	candela/m^2	cd/m^2
FORCE and PRESSURE or STRESS				
lbf	poundforce	4.45	newtons	N
lbf/in^2	poundforce per square inch	6.89	kilopascals	kPa

Technical Report Documentation Page

1. Report No.	2. Government Accession No.	3. Recipient's Catalog No.
4. Title and Subtitle Confinement Effect of Metal Railing Narrow Baseplates on Adhesive Anchor Breakout Resistance		5. Report Date August 2019
		6. Performing Organization Code
7. Author(s) Nakin Suksawang		8. Performing Organization Report No.
9. Performing Organization Name and Address Florida Institute of Technology 150 W. University Blvd Melbourne, FL 32901		10. Work Unit No. (TRAIS)
		11. Contract or Grant No. BDV28 TWO 977-06
12. Sponsoring Agency Name and Address Research Center State of Florida Department of Transportation 605 Suwannee Street, M.S. 30, Tallahassee, Florida 32399-0450		13. Type of Report and Period Covered Final Report May 2017 – July 2019
		14. Sponsoring Agency Code

15. Supplementary Notes
The FDOT Project Manager was Steven Nolan, P.E.

16. Abstract
An updated AASHTO LRFD Bridge Design Specification introduces a new provision for the design of anchors that borrows from the American Concrete Institute Building Code Requirements for Structural Concrete (ACI 318-14). Unfortunately, the ACI 318-14 adhesive anchor design provisions are very conservative by not taking the compressive confinement effect into consideration. The primary objectives of the Florida DOT sponsored research project BDV28 977-06 were to determine the confinement effect of a narrow baseplate on adhesive anchor breakout resistance and develop a new confinement modification factor. Results indicate that the compression confinement from the baseplate significantly increases the concrete breakout resistance. A new confinement modification factor has been developed to address the increase in concrete breakout resistance.

17. Key Word	18. Distribution Statement
adhesive anchors, narrow baseplate, metal rails, connections, confinement modification factor.	No Restriction

19. Security Classif. (of this report)	20. Security Classif. (of this page)	21. No. of Pages	22. Price
Unclassified	Unclassified	44	

Form DOT F 1700.7 (8-72) Reproduction of completed page authorized

ACKNOWLEDGEMENTS

The author would like to thank the direction and support provided by the FDOT project manager, Mr. Steven Nolan and the structural office personnel, Ms. Cheryl Hudson. Additionally, the author would like to recognize the FDOT Structural Research Center, particularly Ms. Christina Freeman and her team for their assistance with the fabrication and testing of the gravity wall test specimens. Finally, the author greatly appreciates the contribution to the experimental program by Florida Tech undergraduate and graduate students, namely Mr. Christopher Peterson, Mr. Josh Perry, Mr. Quinn Daffy and Mr. Paul Ryan.

EXECUTIVE SUMMARY

A new Section 5.13—a provision for the design of anchors—has been added to an updated 2016 AASHTO Bridge Design Specification. This new section borrowed the same specification from ACI 318-14, Chapter 17, which addresses typical anchoring to concrete including adhesive anchors used for standard metal pedestrian/bicycle railings in Florida. Despite being more conservative, this new Section 5.13 will be eventually adopted by the Florida Department of Transportation (FDOT) replacing the current FDOT criteria for the design of adhesive anchors specified in the Structures Manual, Volume 1 (SDG) Section 1.6.

One major criticism of the new Section 5.13 is the ACI 318-14 design criteria assume direct tension. However, in many column-to-foundation connections including the connection for standard metal pedestrian/bicycle railings, the loading is not strictly tension but rather a bending moment—a moment couple of a tensile force in the adhesive anchor and a compressive force from the baseplates in the concrete breakout cone. This confinement effect has shown by previous research to increase the adhesive anchor breakout resistance significantly.

This research project addresses the following primary objectives:

1. Review and identify the effect of confinement of metal railing narrow baseplates on adhesive anchors breakout resistance;
2. Determine the failure mechanism and appropriate confinement modification factor of adhesive anchors used in metal railing;
3. Develop designs for standard metal railings with reduced edge distance and embedment for sidewalks and gravity walls;
4. Develop recommendation for general design procedure modifications to be expanded for other structural applications.

The following tasks were conducted as part of this research project: 1) Literature search on the confinement effect of metal baseplate on adhesive anchor breakout resistance; 2) Development of an experimental program to evaluate the confinement effect of narrow baseplate on adhesive anchors; 3) Fabricate and test concrete block and gravity wall specimens; 4) Develop and propose new confinement modification factor to increase the adhesive anchor resistance; 5) Edit and modify the current design standard with smaller embedment length; and 6) Provide recommendation for general design procedure to be expanded for other structural applications.

The experimental program was divided into three testing schemes. Scheme 1 and 2 were developed to evaluate the confinement effect and embedment length on adhesive anchor resistance. The different between the two schemes was the specimen type, where rectangular concrete blocks representing concrete pavement were used in Scheme 1 and 3 ft gravity walls were used in Scheme 2.

Scheme 3 was developed to evaluate the confinement effect, embedment length and reduced edge distance on adhesive anchor resistance. Rectangular blocks were also used in Scheme 3.

Results indicated that the confinement effect in narrow metal baseplate increased the adhesive anchor breakout resistance by as much 182% when comparing to the ACI 318-14 design criteria. This was especially true for specimens with reduced edge distances, which is often the case in practice. The observed failure mechanism for the concrete block specimen (concrete pavement) resembled a pry-out failure with shear and tension cracks, whereas a concrete cone failure was observed for gravity wall specimens. Overall, the adhesive breakout capacity had a closer match with the ACI 318-14 nominal concrete breakout capacity. A new confinement modification factor (Ψ_m) was developed and proposed to be used with the ACI 318-14 concrete breakout capacity when designing adhesive anchors.

The following recommendations and conclusions could be made:

1. The failure mode of adhesive anchors installed in pedestrian railing with narrow baseplates closely matched the concrete breakout failure mode, and therefore, the concrete breakout failure resistance equation provided by ACI should be used when computing the adhesive anchor resistance.
2. Other than the gravity wall with 12-inch anchor embedment length, no adhesive failure had been observed despite all equations using both SDG and ACI procedures predicted adhesive failure mode. This observation was made even with the use of the lowest strength adhesive that is FDOT approved. Thus, both equations are too conservative and should be omitted when evaluating adhesive anchor with confinement effect provided that the adhesive has an uncharacteristic strength of 940 psi or higher.
3. It is recommended that FDOT modifies the Design Standard, Index 852 & 862 (now Standards Plans Index 515-052 & 515-062) to allow for a reduced embedment length of 6 inches for sidewalk and 9 inches for gravity wall. This would provide significant cost saving and possibly improve quality as large embedment length is challenging and time consuming to install in the field.
4. It is also recommended that FDOT adopts the proposed confinement modification factor, Ψ_m, that can be applied to either the current SDG adhesive bond resistance or ACI concrete breakout resistance to improve the accuracy of the design for adhesive anchor with confinement effect.
5. It is also recommended that FDOT develop a pool fund with AASHTO to investigate the validity of the concrete splitting modification factor, Ψ_{cp}, as this factor significantly reduces the concrete breakout and adhesive bond resistances by as much as 50% which does not seem to be supported by the limited test results in this study.
6. As the scope of this research project is limited to Simpson Strong Tie ET-HP epoxy adhesive, more research is needed to investigate other FDOT approved products that do not meet ICC-ES certification, i.e., products that

met FDOT Method of Test FM-5-568 considering that these products will not meet the new AASHTO specification.

7. It is possible that the proposed general design procedure can also be used in screw anchors. Using screw anchors can further reduce the installation cost and time as there is no additional adhesive cost and no need to wait for the adhesive to harden.

TABLE OF CONTENT

LIST OF TABLES

LIST OF FIGURES

1. CHAPTER ONE – INTRODUCTION

1.1 INTRODUCTION

The Florida Department of Transportation (FDOT) uses adhesive anchor systems to fasten standard metal pedestrian/bicycle railings onto concrete sidewalks, bridges, curbs, and retaining wall copings. Typically, a single $^{7}/_{8}$-inch diameter anchor with an embedment length of 9 inches is used to secure an 8-inch × 6-inch base plate. To accommodate the 9 inches embedment, the 4-inch sidewalk needs to be deepened by tapering the slab at 45 degrees to create a 12-inch × 9-inch (thick × width) edge beam. Figure 1 illustrates the cross section of the sidewalk with installed metal railings. Furthermore, the current specified edge distance of 6 inches also requires the edge beams to be at least 9 inches wide. Therefore, there would be significant cost saving in the materials and construction if these two requirements could be reduced.

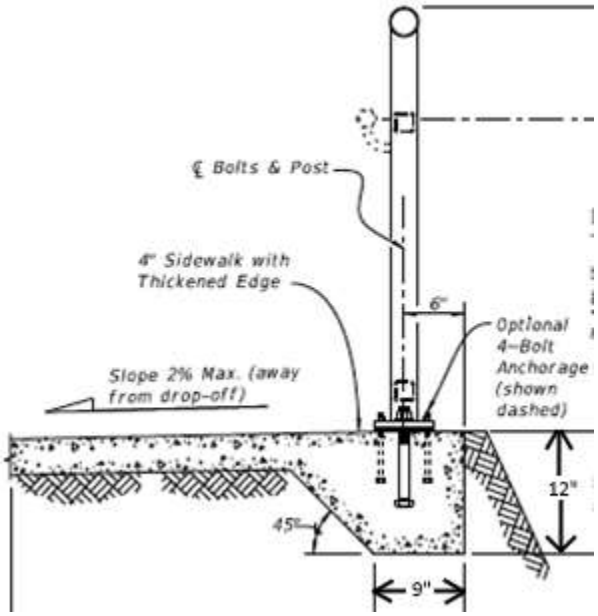

Figure 1—Typical section on concrete sidewalks from Design Standard Index 852 sheet 8 of 8 (FDOT, FY2016-2017)

1.2 PROBLEM STATEMENT

An updated AASHTO Bridge Design Specification introduces a new provision for the design of anchors as described in section 5.13. (AASHTO, 2016) This new provision will eventually replace the FDOT design guidelines for adhesive anchor systems that are specified in the Structural Manual, Volume 1 (SDG), Section 1.6 [FDOT, 2017]. The problem with the new AASHTO provision is that it borrows the same specification from Chapter 17 of the ACI 318-14 Building Code Requirements for Structural Concrete (ACI 318, 2014).

Unfortunately, this would significantly impact FDOT should the new AASHTO be adopted as FDOT will need to make significant changes to the current-state-of-the-

practice. Unlike other States, Florida has its own design (SDG 1.6) and material (FDOT Standard Specification, Section 937) specifications, as well as testing method (FM-5-568) for product qualification for adhesive anchors that were developed as part of two major research initiatives between FDOT and the University of Florida under the direction of Prof. Cook [Cook et al, 1996 and 2002]. Furthermore, ACI 318-14 is more conservative than the design guidelines for adhesive anchor systems provided in the SDG. Therefore, there is a need to investigate the impact of the new provision on adhesive breakout resistance as a pedestrian railing fastening system.

Moreover, although the ACI 318-14 design criteria reflects the failure mechanisms of adhesive anchor systems, it ignores the compression confinement in the concrete cone breakout area provided by the metal railings' base plate. In many column-to-foundation connections, the loading is not strictly tension but rather a bending moment. The bending moment at the connection transfers both the bending compressive force from the base plate to the concrete foundation and the tensile force through the adhesive anchor as illustrated in Figure 2. In the figure, z is the internal moment arm calculated in accordance with elastic theory and h_{ef} is the anchor embedment length. This compression confinement has been shown to increase the concrete cone breakout capacities and could potentially increase the design capacity for adhesive anchor systems, which would permit a shorter embedment length (Zhao, 1993).

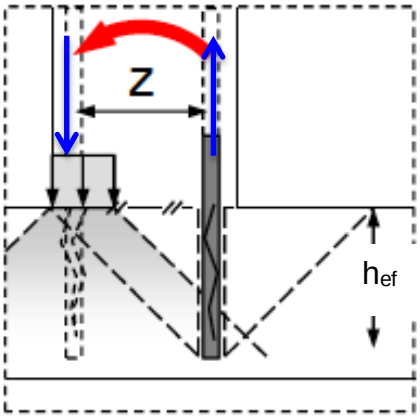

Figure 2—Effect of moment on standard metal pedestrian/bicycle railings connections as adopted from Eligehausen et al (2014)

The SDG addresses the confinement effect by multiplying the design tensile bond strength for adhesive anchor with a concrete breakout strength modification factor, Ψ_m. The factor Ψ_m corresponds to the experimental moment capacity divided by the calculated moment capacity based on concrete breakout capacity, which was first introduced by Zhao (1993). The factor Ψ_m specified in the SDG is based on a non linear equation proposed by Fichtner (2011) and recommended by Eligehausen et al (2006), and ranges from 1.0 to 2.5 depending on the z/h_{ef} ratio (the moment arm to the anchor embedment length ratio). The smaller the z/h_{ef} ratio is, the higher value factor Ψ_m

becomes. Standard metal railings have narrow base plates; therefore, the z/h_{ef} ratio would not exceed 0.33 and $\Psi_m \geq 1.875$ for an embedment length of 9 inches. This is in a significant increase in design tensile bond strength for adhesive anchor base plate system.

1.3 SCOPE

The scope of this research project is limited to the investigation of the performance of $^7/_8$ in adhesive anchors embedded in non-structural (Class NS) concrete. The investigation included two types of concrete structures, namely concrete pavement and gravity wall. Only a 42-inch steel pedestrian railing that was fabricated in accordance with FDOT Design Standard, Index 852 (now Standard Plans Index 515-052) were used in this investigation [FDOT, 2019]. The adhesive is also limited to Simpson Strong Tie ET-HP epoxy adhesive as it is the lowest-strength product on the FDOT Approved Products list with ICC-ES certification to also satisfy ACI 355.4 criteria for adhesive anchors.

1.4 OBJECTIVES

Four primary objectives were identified for this research project:

1. Review and identify the effect of confinement of metal railing narrow baseplates on adhesive anchors breakout resistance;
2. Determine the failure mechanism and appropriate confinement modification factor of adhesive anchors used in metal railing;
3. Develop designs for standard metal railings with reduced edge distance and embedment for sidewalks and gravity walls;
4. Develop recommendation for general design procedure modifications to be expanded for other structural applications.

2. CHAPTER 2 – BACKGROUND

2.1 INTRODUCTION

An overview of the behavior of adhesive anchor systems, particularly their failure mechanism and the effect of confinement of connection base plate on post-installed adhesive anchors breakout resistance are presented in this section. Section 2.2 describes a review of the three main failure mechanisms of adhesive anchor systems. A summary of ACI 318-14 design criteria for different failure mechanisms are also provided in this section. Section 2.3 of the report examines the effect of the compression confinement on the concrete breakout resistance. Several confinement modification factor equations are also presented here. Section 2.4 gives a background on the effects of edge distance on adhesive anchor breakout resistance and how these effects are accounted for in ACI 318-14. Finally, a summary of the literature review on adhesive anchor systems is provided in Section 2.5.

2.2 FAILURE MECHANISM

There are three main failure mechanisms for single adhesive anchors loaded in tension. These three failure mechanisms consist of 1) concrete cone failure, 2) pullout failure, and 3) steel failure. The pullout failure could also be further broken into three

subcategories of failure modes consisting of i) bond failure in the concrete, ii) bond failure in the adhesive, and iii) mixed bond failure in the concrete and adhesive. Figure 3 illustrates a summary of all possible failure mechanisms of single adhesive anchor systems loaded in tension.

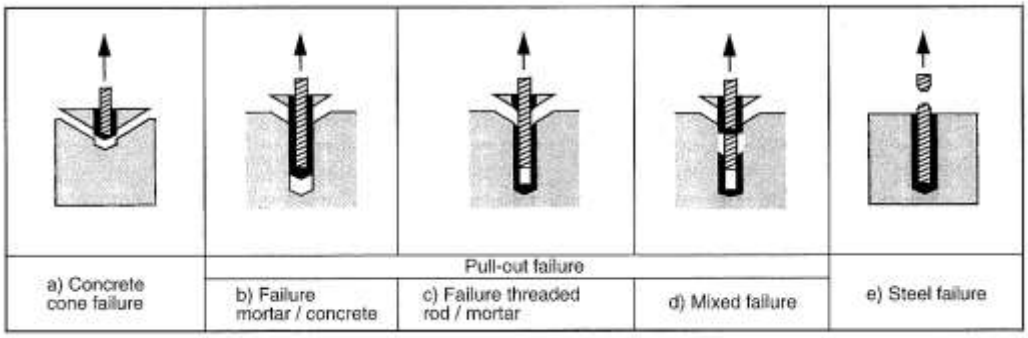

Figure 3—Failure mechanism of adhesive anchor systems (Cook et al, 1998)

2.2.1 Concrete Cone Failure

The concrete cone failure is typically found in adhesive anchor systems loaded in tension with small embedment lengths defined as between 3 and 5 times the diameters of the anchoring rods (Eligehausen et al, 2006). It is characterized by a cone-shaped concrete breakout originating from the anchor base propagating at approximately 35 degrees slope with respect to the concrete surface. For larger embedment length the failure mode transitions into mixed failure mode of adhesive bond and concrete breakout, which is the most common type of failure in adhesive anchor systems (Cook et al, 1998).

While pure concrete cone failure may not be typical mode of failure in adhesive anchor systems, it does serve as an upper bound for the design (Cook et al, 1998; Zamora et al, 2003; Eligehausen et al, 2004, 2006). This is especially true when low strength concrete ($f_c' \leq$ 3,000 psi), large anchor diameter, and high characteristic bond strength adhesive ($\tau_{uncr} >$ 1800 psi) are used. Table 1 summaries a list of FDOT approved adhesives and their characteristic bond strength for $^{7}/_{8}$-inch diameter anchors used with uncracked concrete at normal temperature range. From this list, only the Simpson Strong Tie ET-HP epoxy adhesive, which has the lowest characteristic bond strength, was investigated. It should be noted that the SDG does not take the concrete cone failure into the design consideration but the ACI 318-14 does.

The ACI 318-14 concrete cone breakout model is based on a model proposed by Fuchs et al (1995) for cast-in-place and post-installed mechanical anchor systems. This model is based on a k-factor (denoted as k_c in ACI 318-14) multiply by the square root of the concrete compressive strength and embedment length raised to a power. According to ACI 318-14, the concrete breakout capacity for single cast-in-place and post-installed mechanical anchors in uncracked concrete is given by the following equation:

$$N_b = k_c \lambda_a \sqrt{f_c'} h_{ef}^{1.5} \quad \text{Eq. 1}$$

where λ_a is the modification factor to reflect the reduced mechanical properties of lightweight concrete, f'_c is the concrete compressive strength, and h_{ef} is the embedment length. The k_c is a constant depending on whether cast-in-place or post-installed mechanical anchors are used as the cast-in-place anchors produce failure loads approximately 15% higher than those of post-installed anchors. The k_c values recommended by Fuchs et al (1995) were based on the mean concrete breakout capacity whereas the values adopted by ACI 318-14 were based on 5% fractile of the concrete breakout capacity using a coefficient of variation of 0.15 and 0.20 for cast-in-place and post-installed mechanical anchors, respectively. As a result, there is a significant difference between the mean k_c values and the values provided by ACI 318-14, i.e., for post-installed mechanical anchors, the mean k_c is 35 whereas 17 is specified by the ACI 318-14. However, ACI 318-14 does permit a higher k_c value but limits it to a maximum value of 24 for post-installed mechanical anchors. The reason for ACI 318-14 choosing 5% fractile for the design of anchor systems is to account for several influencing factors on anchor performance such as the variability in the installation procedures, increased temperature, and long-term behaviors.

Currently, the assumption is that the k_c value for adhesive anchors would match the value used for post-installed mechanical anchors considering that there is not a significant different between the concrete cone failure loads between torque-controlled expansion anchors and drop-in anchors (Eligehausen et al, 2006). Analysis of existing data indicated that the failure load is either slightly below or equal to the mean concrete breakout capacity proposed by Fuchs et al (1995) using the mean k_c value. The question is whether this assumption is also true for adhesive anchor systems. Furthermore, another question is if the 5% fractile value could be increase to 24 or even higher to allow for lower embedment length and shorter edge distance considering that FDOT has stricter material specification than ACI 318-14. These questions need to be further investigated but are beyond the scope of this project as this would require significant amount of data (possibly from the manufacturers and published and unpublished reports) and/or a more comprehensive experimental program.

Table 1– Characteristic Bond Strength for Uncracked Concrete of FDOT Approved Products with ICC-ES certification

ESR#	**Product Names**	**τ_{uncr} (psi) 7/8" rod**
3372	Simpson ET-HP *(Type HV & HSHV)*	940
1137	ITW Red Head G5	1155
3187	Hilti HIT-HY 200-R	1560
3829	Hilti HIT-RE 100	1124
3814	Hilti HIT-RE 500 V3	2040
3298	Dewalt-Powers Pure100+	1567
3576	Dewalt-Powers Pure50+	1357

To make the ACI 318-14 even more conservative, despite the model using the 5% fractile concrete breakout strength to obtain k_c, other factors including the effects of multiple anchors, spacing of anchors, and edge distance on the concrete breakout capacity are also included by applying modification factors A_{Nc}/A_{Nco}, $\Psi_{ed,N}$, $\Psi_{c,N}$, $\Psi_{cp,N}$. As a result, the nominal concrete breakout capacity for single anchor becomes:

$$N_{cb} = \frac{A_{Nc}}{A_{Nco}} \Psi_{ed,N} \Psi_{c,N} \Psi_{cp,N} N_b \qquad \text{Eq. 2}$$

where the A_{Nc}/A_{Nco} is a ratio of the total projected area of the anchor to the maximum projected area for single anchor as illustrated in Figure 4. $\Psi_{ed,N}$ is a modification factor to account for the edge distance, $\Psi_{c,N}$ and $\Psi_{cp,N}$ are modification factors to account for concrete cracking and the potential for concrete splitting failure prior to concrete breakout failure.

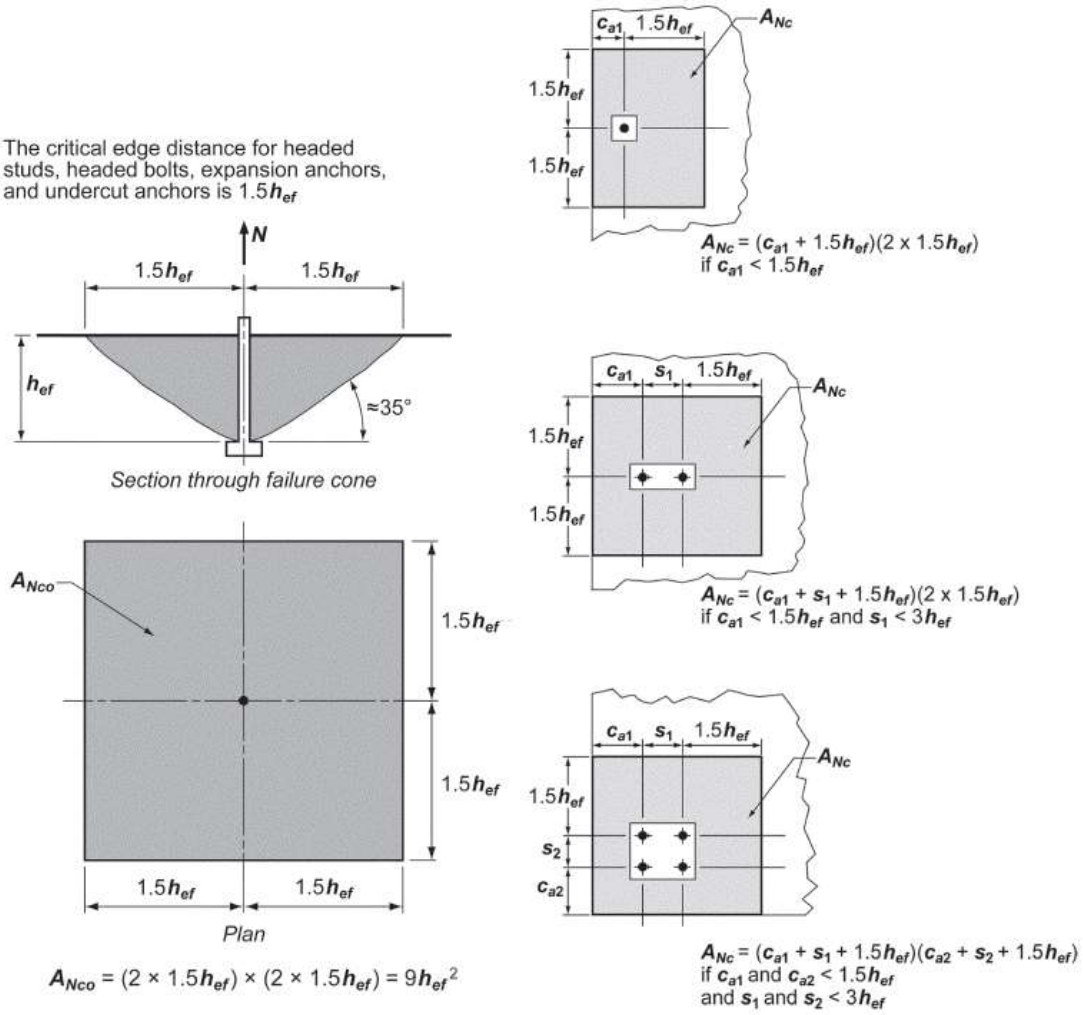

Figure 4—Examples of various concrete breakout failure projected area for single and group anchors (ACI 318, 2014)

2.2.2 Pullout Failure

As stated earlier there are three subcategories of failure modes within the pullout failure. These modes make it difficult to predict the pullout failure loads since the load transfer mechanism at the bond interfaces between the adhesive/concrete, steel/adhesive, and the mixed failure interfaces are different. There are many influential factors such as concrete compressive strength, adhesive bond strength, hole preparations, and concrete temperature, which all play important roles in the pullout capacity of the adhesive anchor systems. However, their relationships with the pullout failure loads may not be directly proportional.

For example, earlier pullout capacity models related the pullout failure loads with the square root of the concrete compressive strength (Eligehausen et al, 1984; Cook, 1993). This seems logical considering that higher concrete compressive strength would also increases the bond strength, however, as the concrete strength increases, the sides of the drilled holes also become smoother resulting in no net gain in pullout capacity. The pullout capacity also depends on the hole's preparation. Failure to remove drilling dust and concrete fragment could reduce the pullout capacity up to 80% (Meszaros, 1999). The type of adhesive also plays an important role since some adhesive bond strengths fluctuate with temperature variation and anchor's diameter (Cook et al, 1998). A complete overview of all factors contributing to pullout capacity can be found in Davis's Ph.D. thesis (Davis, 2012). All these factors make the pullout behavior difficult to model and predict.

The actual stress distribution along the embedment length of the anchor rod is nonlinear (Eligehausen et al, 2004). As illustrated in Figure 5, the shear stress distribution varies significantly along the embedment length. However, to simplify the model either hyperbolic tangential or uniform stress distribution is used as respectively illustrated in Figures 6a and 6b. For the hyperbolic tangential stress distribution model, the maximum bond stress is used, whereas, the mean bond stress is used in the uniform stress distribution model.

McVay et al (1996) examined two pullout models for the design of adhesive anchors. The first was the elastic bond-stress model proposed by Cook at al (1993), which appears to be appropriate for large embedment lengths. The second model uses uniform bond stress, which is simpler to apply while providing good correlation between the predicted and measured pullout capacities. ACI 318-14 adopted the uniform bond stress model, which is also the model currently specified in the SDG (see Eq. 1-4 in the SDG). The uniform bond stress model is given by ACI 318-14 as:

$$N_{ba} = \lambda_a \tau_{uncr} \pi d_a h_{ef} \qquad \text{Eq. 3}$$

where λ_a is the modification factor to reflect the reduced mechanical properties of lightweight concrete, τ_{uncr} is the characteristic bond strength of the adhesives in uncracked concrete using 5% fractile bond strength in accordance with ACI 355.4, d_a is the anchor diameter, and h_{ef} is the anchor embedment length.

Although for design purpose using 5% fractile bond strength is appropriate to account for various variables affecting bond strength, using the mean adhesive bond strength would be more appropriate in later task to investigate the confinement effect from the metal railing base plate. It is important that if new models or modification factors were to be developed, models reflecting actual behaviors of the adhesive anchor breakout resistance should be used. The 5% fractile could be applied later to ensure that the proposed model would satisfy ACI 318-14 and ACI 355.4 safety criteria.

There are also other pullout models for adhesive anchor that are summarized in Cook (1993), Cook et al (1998), and Eligehausen et al (2006). Some of these models are more complex and not suited for design so they are not discussed here. Furthermore, proposing new models for pull out failure is beyond the scope of the project. The project will focus on developing new or proposing existing modification factors (i.e., factor Ψ_m and c_{Na}) that would permit the design of adhesive anchor systems with a smaller embedment length and edge distance.

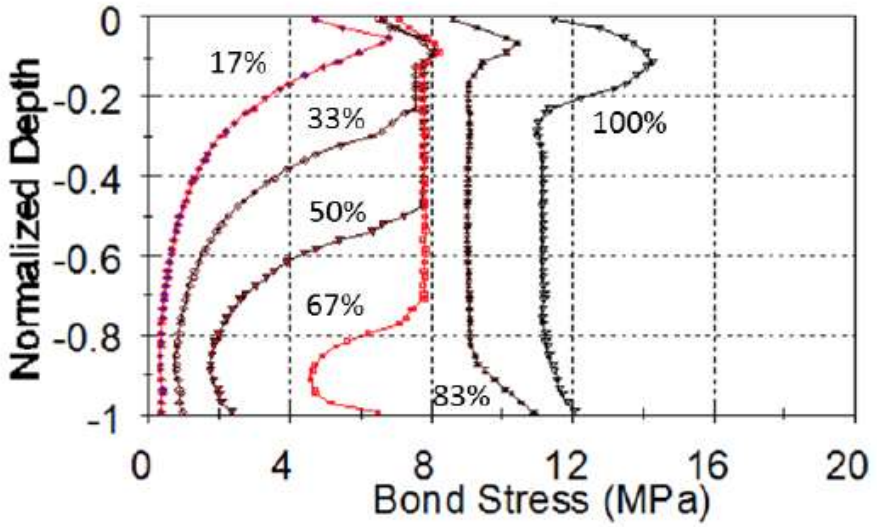

Figure 5—Shear stress development along concrete/adhesive interface (McVay et al, 1996)

To determine the nominal pullout capacity, Eq. 3 is multiplied by various modification factors to account for the influence of anchor spacing and edge distance, influence area, and concrete cracking. The nominal pullout capacity is given by:

$$N_a = \frac{A_{Na}}{A_{Nao}} \Psi_{ed,Na} \Psi_{cp,Na} N_{ba} \qquad \text{Eq. 4}$$

where the A_{Na}/A_{Nao} is a ratio of the total projected influence area associate with bond strength of the adhesive anchor group to the projected influence area associate with bond strength of a single adhesive anchor as illustrated in Figure 7. $\Psi_{ed,Na}$ is a modification factor to account for the edge distance, and $\Psi_{cp,N}$ is a modification factor to account for cracked concrete.

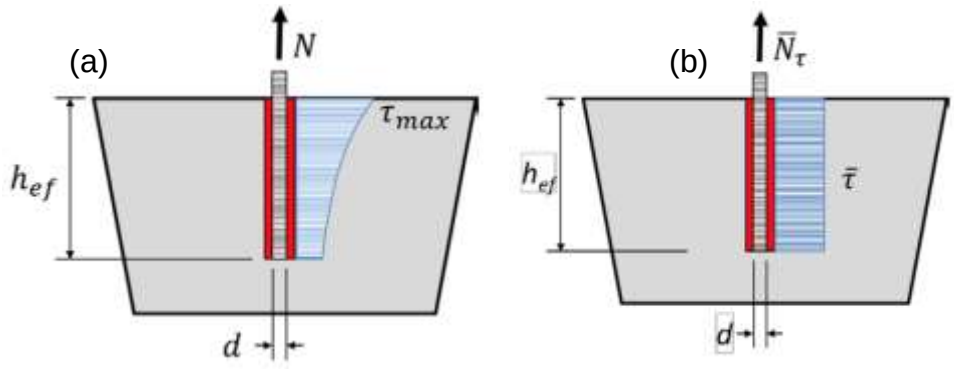

Figure 6—Modeling bond behavior using a) Hyperbolic tangential stress distribution and b) uniform stress distribution (Davis, 2012)

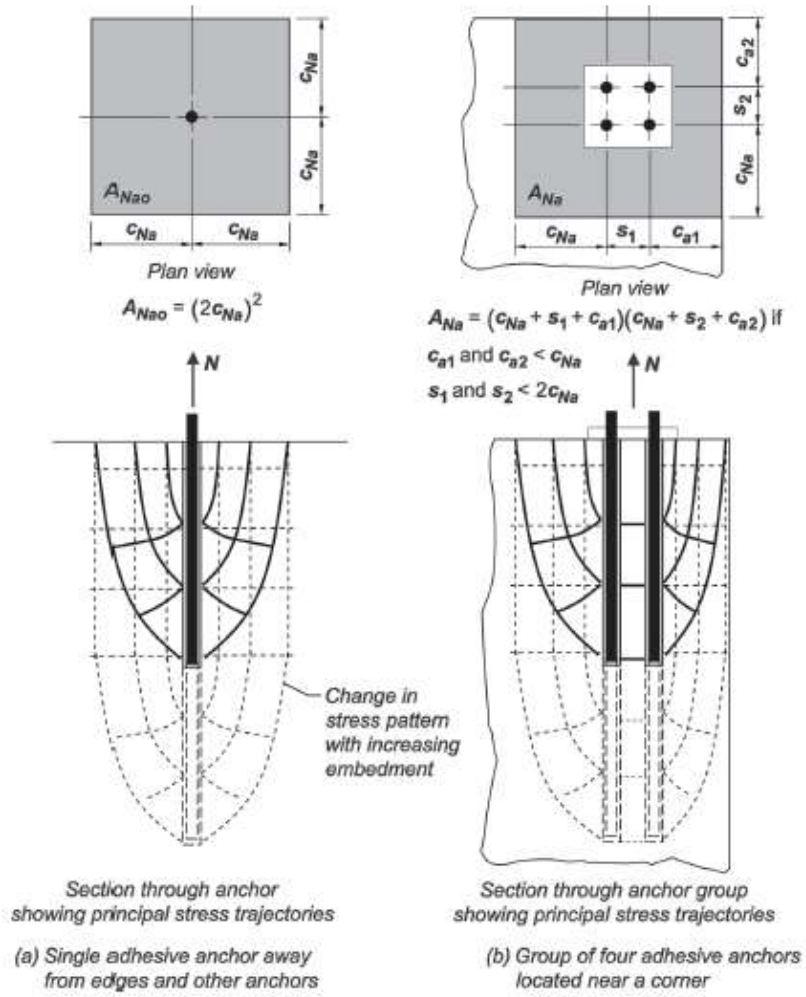

Figure 7—Projected influence area associate to bond strength for adhesive anchor (ACI 318, 2014)

It should be noted that the c_{Na} in Figure 7 is not the same as 8d (8 times the anchor diameter) currently specified in the SDG and given as:

$$c_{Na} = 10d\sqrt{\frac{\tau_{uncr}}{1100}} \qquad \text{Eq. 5}$$

Considering that with the exception of Simpson ET-HP, the projected influence area associate to bond strength for a single anchor would be much higher using ACI 318-14 than SDG, which would result in a higher reduction in nominal pullout capacity using the equation provided by ACI 318-14.

2.2.3 Steel Failure

Steel failure is based on the rupture of the anchor rod, where the ultimate load can be calculated from the stressed cross-sectional area and ultimate tensile strength of steel. The ACI 318-14 steel rupture equation is given by the following equation:

$$N_{sa} = A_{se,N} f_{uta} \qquad \text{Eq. 6}$$

where f_{uta} is the ultimate tensile strength of the anchor rod but should not exceed either 1.9 times its yield strength or 125,000 psi. These limits were imposed on f_{uta} to ensure that under service load condition, the stress in the anchor would not exceed the yield strength. $A_{se,N}$ is the effective cross-sectional area specified by the manufacturers or defined by ASME B1.1 (ASME, 2003) for threaded rod as:

$$A_{se,N} = \frac{\pi}{4}\left[d_a - \frac{0.9743}{n_t}\right]^2 \qquad \text{Eq. 7}$$

where d_a is the gross diameter of the threaded rod and n_t is the number of threads per inch. Equations 6 and 7 are slightly different than the current SDG that defines steel failure as the yielding of the anchor rods and the effective cross-sectional area is defined as 75% of the gross area of the threaded rod. Considering the different failure criteria, the SDG specifies a value of 0.9 for the resistance factor whereas the ACI 318-14 uses 0.75. Despite their differences between the SDG and ACI 318-14, for shallow embedment length (as the project aims to decrease the embedment length) the steel failure mode will never control the design loads.

2.3 CONFINEMENT EFFECT

According to Zhao (1993) the confinement effect on concrete breakout resistance depends on the internal moment arm, z, between the resultant tension and compressive forces as illustrated in Figure 2. If z is smaller than $1.5h_{ef}$ (i.e., the resultant compressive force is acting within the projected cone failure area) then the resultant compressive force on the railing base plate will increase the concrete breakout capacity. However, if z were greater than $1.5h_{ef}$ then there would not be any influence on the confinement on the concrete breakout resistance. The internal moment arm, z, is calculated according to elastic theory assuming stiff base plates.

The increase in the concrete breakout strength is addressed by applying a modification factor, Ψ_m, which correspond to the experimental moment capacity divided by the calculated moment capacity based on concrete breakout capacity. This modification factor is applied to Eq. 2. The factor Ψ_m is based on experimental tests of groups with four and nine headed anchors under tension force, bending moment and shear force in one direction performed by Zhao (1993). Figure 8 illustrates the test schematic used by Zhao (1993) who also proposed an equation to represent factor Ψ_m as follows:

$$\Psi_m = \frac{1.5h_{ef}}{z} \qquad \text{for } 0 \leq \frac{z}{h_{ef}} \leq 1.5 \qquad \text{Eq. 8a}$$

$$\Psi_m = 1 \qquad \text{for } \frac{z}{h_{ef}} > 1.5 \qquad \text{Eq. 8b}$$

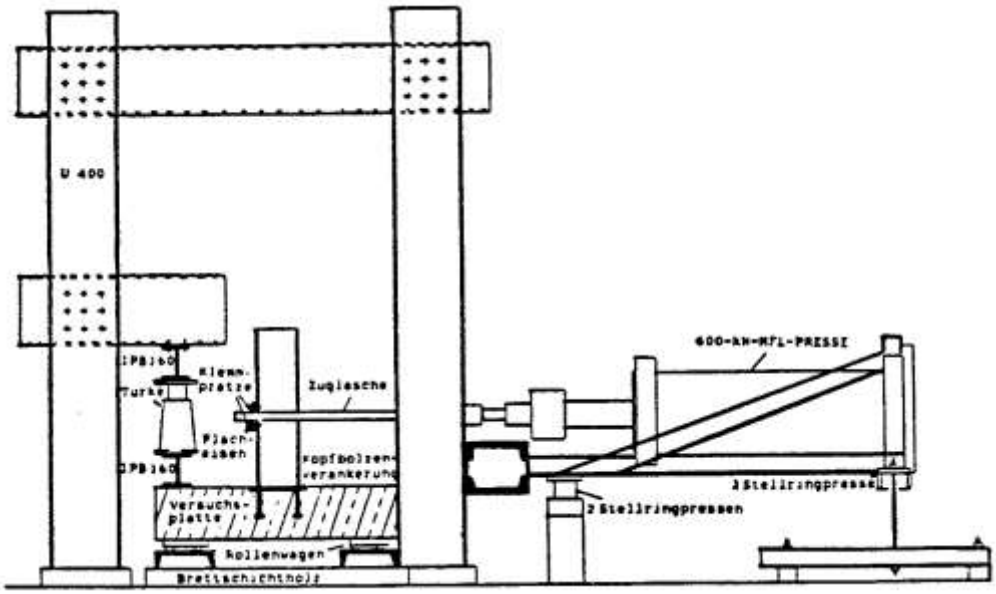

Figure 8—Testing schematic for groups with four and nine headed anchors under tension force, bending moment and shear force in one direction (Zhao, 1993)

To improve the model for factor Ψ_m, more tests were conducted by Varga and Eligehausen (1995, 1996) for groups with four, six, and nine headed anchors but under tension force and bending moment in one direction as well as under tension force and bending moment in two directions (i.e., biaxial bending moment) as illustrated in Figure 9. Additionally, Bruckner et al (2001) developed a nonlinear finite element model to analyze the behavior of groups with four anchors under bending moment in one direction and proposed a more conservative factor Ψ_m as follows:

$$\Psi_m = 2 - \frac{z}{h_{ef}} \qquad \text{for } 0 \leq \frac{z}{h_{ef}} \leq 1.0 \qquad \text{Eq. 9a}$$

$$\Psi_m = 1 \qquad \text{for } \frac{z}{h_{ef}} > 1.0 \qquad \text{Eq. 9b}$$

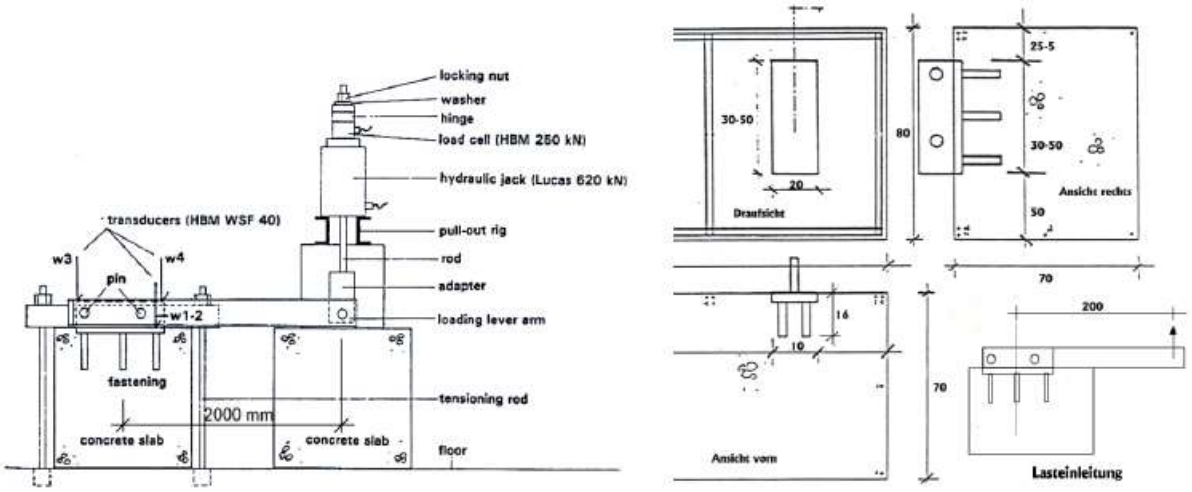

Figure 9— Testing schematic for groups with six headed anchors under tension force and bending moment in one direction (Varga and Eligehausen, 1995,1996)

More tests were then carried out by Eligehausen et al (2008) on groups with 4, 6, and 9 headed anchors under tension and bending moment in one and two directions using similar test setup as Varga and Eligehausen (1995, 1996) but with more modern instrumentation as shown in Figure 10.

Using all these test results, Fichtner (2011) proposed two equations for the factor Ψ_m, one of which is currently being used in the SDG as shown in equations 10a and 10b, and another linear equation shown in equations 11a and 11b.

$$\Psi_m = \frac{2.5}{1+\frac{z}{h_{ef}}} \qquad \text{for } 0 \le \frac{z}{h_{ef}} \le 1.5 \qquad \text{Eq. 10a}$$

$$\Psi_m = 1 \qquad \text{for } \frac{z}{h_{ef}} > 1.5 \qquad \text{Eq. 10b}$$

$$\Psi_m = 2 - \frac{2z}{3h_{ef}} \qquad \text{for } 0 \le \frac{z}{h_{ef}} \le 1.5 \qquad \text{Eq. 11a}$$

$$\Psi_m = 1 \qquad \text{for } \frac{z}{h_{ef}} > 1.5 \qquad \text{Eq. 11b}$$

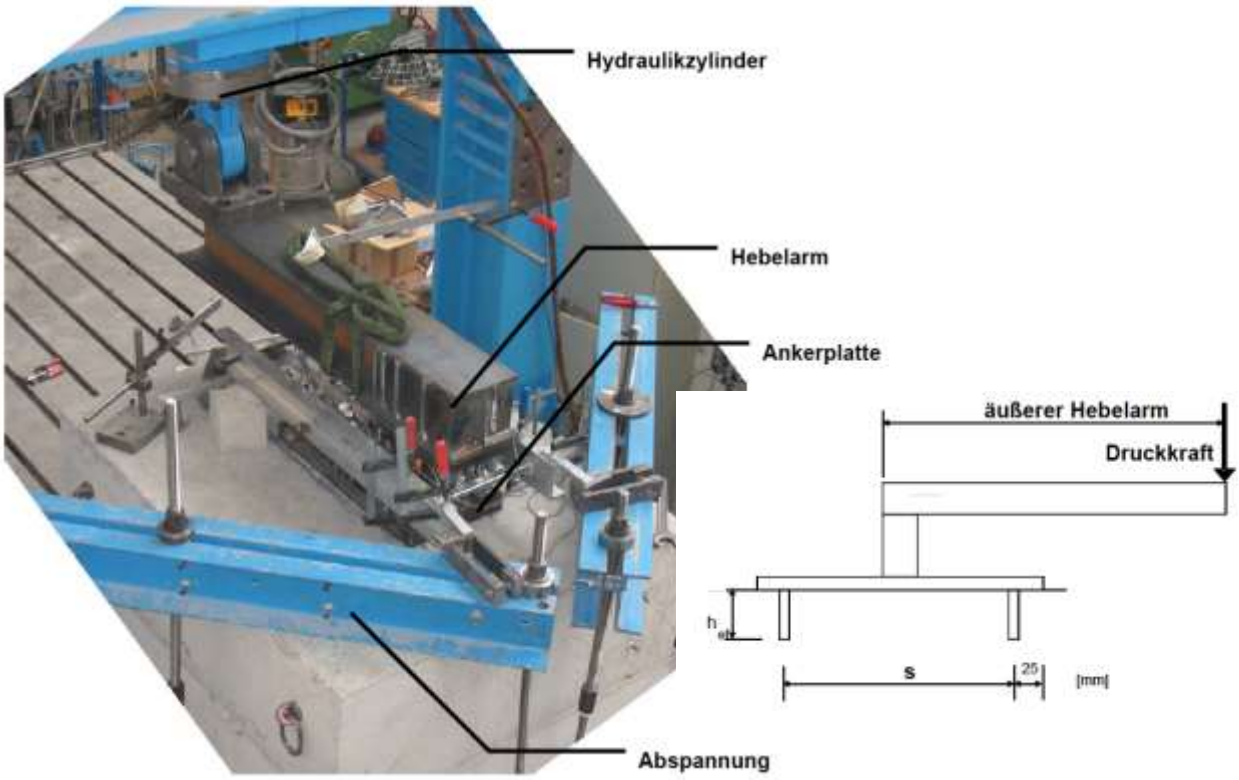

Figure 10—Test setup for groups with four and nine headed anchors subjected to tension force and bending moment in one direction (Fichtner, 2011)

Additionally, Herzog (2015) studied the bond and concrete behavior in the anchorage zone of connections between concrete walls and strip foundation and between concrete columns and spread foundations. These connections were cast-in and post-installed reinforcing bars that transfer the tension force from the structural members to the foundation elements. The test setup used by him is illustrated in Figure 11. He also validated the bond and concrete behavior using nonlinear finite element. Herzog (2015) proposed another equation for factor Ψ_m, which are shown below:

$$\Psi_m = 2.5 - \frac{z}{h_{ef}} \qquad \text{for } 0 \leq \frac{z}{h_{ef}} \leq 1.5 \qquad \text{Eq. 12a}$$

$$\Psi_m = 1 \qquad \text{for } \frac{z}{h_{ef}} > 1.5 \qquad \text{Eq. 12b}$$

All these equations and test results are illustrated in Figure 11. From the figure, it could be observed that there is no test data representing connections with $z/h_{ef} < 0.33$, which is the range for the narrow base plate on metal pedestrian/bicycle railings. Therefore, there is a need to investigate the validity of the available equations for factor Ψ_m. It is important to point out that even though the factor Ψ_m has been developed for concrete breakout failure, Eligehausen et al (2014) have applied this factor to the bond failure as

well but more research is needed to verify the applicability of using the factor Ψ_m with anchor pull out capacity.

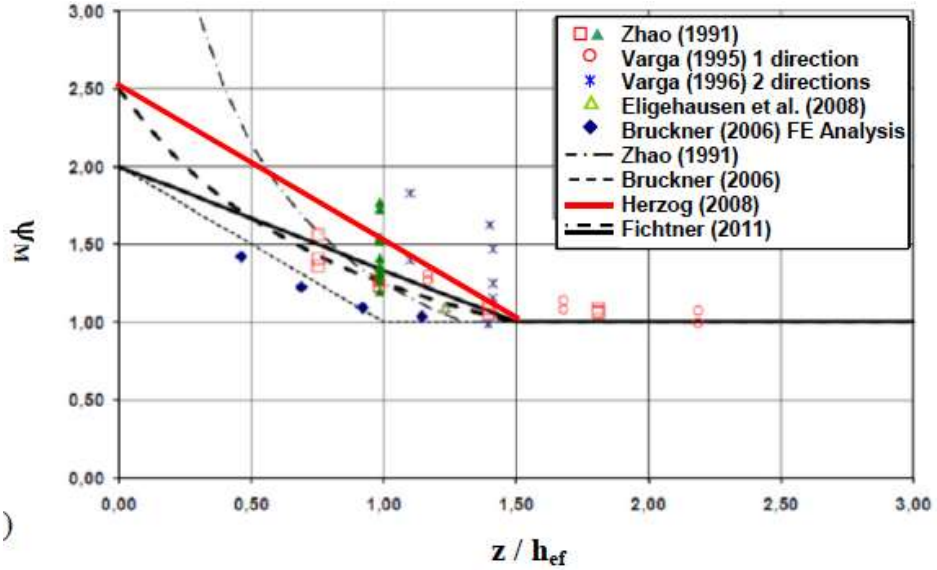

Figure 11—Factor Ψ_m as a function of z/h_{ef} ratio from Eligehausen et al (2014)

2.4. EDGE DISTANCE

As stated earlier, both the concrete cone and adhesive anchor pullout capacities need to be reduced if the projected influence area as shown in Figures 4 and 7 for a single anchor is reduced due to shorter edge distance. Figure 12 illustrates the influence of edge distance on the shape of the concrete cone failure surface. The reduction in the projected influence area is accounted for in both equations 2 and 4 by taking the ratio of the reduced projected influence area (i.e., area shown in figure 12b) by the projected influence area of a single anchor (i.e., area shown in figure 12a). Additionally, these capacities are further reduced by the factor Ψ_{ed} to account for disruption in the rotationally symmetric stress condition with the reduced area as illustrated in Figures 13a and 13b. The general factor Ψ_{ed} is given as:

$$\psi_{ed} = 0.7 + 0.3\frac{c}{c_{cr,N}} \leq 1.0 \qquad \text{Eq. 13}$$

where c is the smallest edge distance and $c_{cr,N}$ is $1.5h_{ef}$ for concrete cone failure or c_{Na} for pullout failure, which is shown in Eq. 5. Equation 5 is based on the recommendation of Eligehausen et al (2005). It should be noted that as there is a wide scatter in the data to develop Eq. 13 as illustrated in Figure 14, several researchers recommended various quantities for $c_{cr,N}$ for pullout failure. Kunz et al (1998) recommended $c_{cr,N} = 0.875h_{ef}$, while Lehr (2003) suggested $c_{cr,N} = 8d$ (8 times the anchor diameter), which is also the specified value in the SDG. Although, one of the objectives for this project is to reduce the edge distance, developing new $c_{cr,N}$ equation is beyond the scope of this project. Considering that ACI 318-14 will be adopted by FDOT, Eq. 5 will be used in the

investigation rather than the current $c_{cr,N}$ = 8d specified in the SDG. The research will put more emphasis on determining the factor Ψ_m.

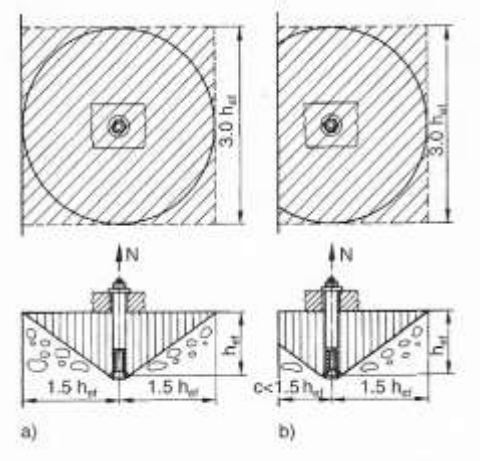

Figure 12—Projected concrete cone failure surface for a single anchor a) away from the edge and b) close to the edge (Eligehausen et al, 2006)

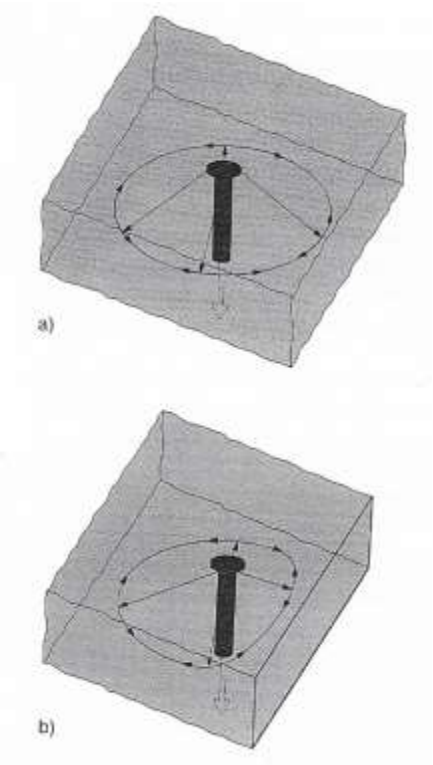

Figure 13—Stress distribution in the concrete anchorage zone a) away from the edge and b) close to the edge (Eligehausen et al, 2006)

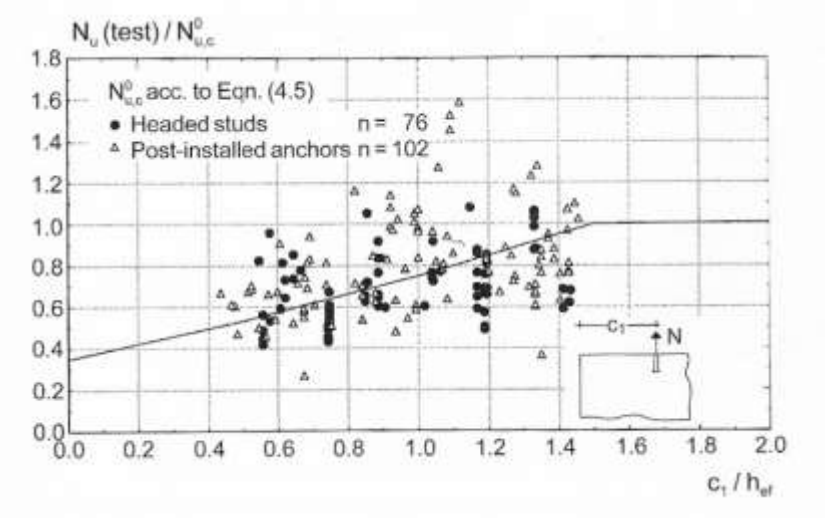

Figure 14—Influence of edge distance on concrete cone failure (Eligehausen et al, 2006)

2.5 SUMMARY

The failure mechanisms of adhesive anchor system are highly complex and very difficult to predict. For anchor subjected to tensile force, the failure mechanisms consist of concrete cone failure, pullout failure, and steel rupture. The BDS, which borrows the specification on adhesive anchor from ACI 318-14, does address these failure mechanisms. However, for column-to-foundation connections including the connection for standard metal pedestrian/bicycle railings, the loading involves bending moment. The bending moment confines the concrete cone breakout area by generating a compressive force under the steel base plate in addition to the tensile force in the anchor. As a result, the confinement increases the adhesive anchor breakout resistance. Hence, the models in the AASHTO would be conservative, as they do not reflect the actual behaviors found in metal railings.

To account for the confinement effect, the factor Ψ_m has been proposed by various researchers and one was also adopted by the SDG. However, the validity of these models for factor Ψ_m on metal railing needs to be further examined since no test data representing connections with $z/h_{ef} < 0.33$ was used in developing these models. Furthermore, the factor Ψ_m was developed as a modification factor for the concrete breakout failure, which may not govern the design if pullout failure controls. Thus, there is a need to determine if the factor Ψ_m is also applicable for the pullout failure mode as well. All these questions will be answered later in this project through an experimental program.

3. CHAPTER THREE – RESEARCH METHODOLOGY

3.1 INTRODUCTION

To address the project objectives, an experimental program was developed and divided into three testing schemes. Scheme 1 was used to evaluate the confinement effect of metal railing narrow baseplates on adhesive anchor breakout resistance without the influence of edge distance. Scheme 2 consisted of testing the performance of post-install adhesive anchors influence by edge effects on a 3-feet tall narrow top gravity wall. Scheme 3 was to evaluate the combined effect of reduced-edge distance and confinement effect on adhesive anchor breakout resistance.

3.2 EXPERIMENTAL PARAMETERS

There are three main experimental parameters that were evaluated: 1) the embedment depth, 2) the edge distance and 3) the longitudinal reinforcement spacing in the gravity wall.

For Scheme 1, the concrete block samples were sized to accommodate the theoretical breakout area of $9h_{ef}$, where h_{ef} is the embedment length. Three embedment lengths of 4, 6 and 9-inches, were evaluated. The 9-inch embedment depth represents the standard embedment depth as specified by the FDOT Design Standards, Index 852 & 862 (now Standard Plans Index 515-052 & 515-062). The 6- and 4-inch are reduced embedment depths. Although the 4-inch embedment depth will not be used in practice, it is included in the experimental program to provide additional data points to help formulate an equation for the confinement modification factor, Ψ_m. Three test specimens were used for each embedment length, totaling nine pullout tests. These embedment lengths were chosen to capture different z/h_{ef} ratios, where z is the internal moment arm between the tension anchor and baseplate compressive reaction resultant, assumed to be 2.5 inches for the FDOT standard 6-inch wide center-bolted railing baseplate. These z/h_{ef} ratios were chosen to help in the evaluation of the confinement modification factor, Ψ_m that is currently used in the SDG but omitted from the ACI318-14, Chapter 17.

For Scheme 2, the testing of the performance of post-install adhesive anchors influence by the gravity wall was evaluated using a standard embedment length of 12 inches and a reduced embedment length of 9 inches. Additionally, the effect of the longitudinal reinforcement restraint in the gravity wall was also evaluated by reducing the center-to-center spacing of the longitudinal reinforcement from standard 18 inches to 12 inches. This was only done on the specimens with reduced adhesive anchor embedment length of 9 inches. As a result of the size of these test specimens, only two test samples were used for each test case.

For Scheme 3, the same test setup as the Scheme 1 was used but with a reduced-edge distances. The evaluated edge distances were the standard 6 inches in accordance with the FDOT Design Standards, Index 852 & 862 (now Standard Plans Index 515-052 & 515-062), 4.5-inches (25% reduction) and 3 inches (50% reduction). The 3-inch edge distance represented the condition when the side of the baseplate is flush against the edge of the concrete slab, and is therefore, the practical minimum edged distance that

could be used for FDOT metal railings. Table 2 provides a summary of the list of experimental parameters. A total of 33 specimens were fabricated and tested in this project.

Table 2: List of experimental parameters

	Scheme 1			Scheme 2		
ID	S9	S6	S4	W12	W9	W9-X
Embedment (in)	9	6	4	12	9	9
z/h_{ef}	0.28	0.42	0.63	0.28	0.42	0.42
Edge Distance (in)	15	10.50	7.50	4.00	4.00	4.00
No. of Specimens	3	3	3	2	2	2
	Scheme 3					
ID	S9-6	S9-4.5	S9-3	S6-6	S6-4.5	S6-3
Embedment (in)	9	9	9	6	6	6
z/h_{ef}	0.28	0.28	0.28	0.42	0.42	0.42
Edge Distance (in)	6	4.5	3	6	4.5	3
No. of Specimens	3	3	3	3	3	3

3.3 TEST SETUP

The test setup involved the application of a lateral force to the top of a metal post using a hydraulic jack such that a moment couple is generated at the baseplate. For Schemes 1 and 3, a self-reacting steel frame, illustrated in Figure 15, was used. The concrete specimen was fastened to the steel frame using steel tubing to prevent the concrete slab from overturning. A load cell was used to record the lateral force exerted by the hydraulic jack to the top of the metal post. The tension force in the adhesive anchors was computed by using elastic theory by dividing the bending moment at the baseplate by z (the internal moment arm between the tension anchor and baseplate compressive reaction resultant).

Similar test setup was used for Scheme 2 testing but rather than using a self-reacting frame, the test setup involved a reaction frame that was tied down to a strong floor. This test was conducted at the FDOT Structural Research Center. Figure 16 illustrates Scheme 2 test setup.

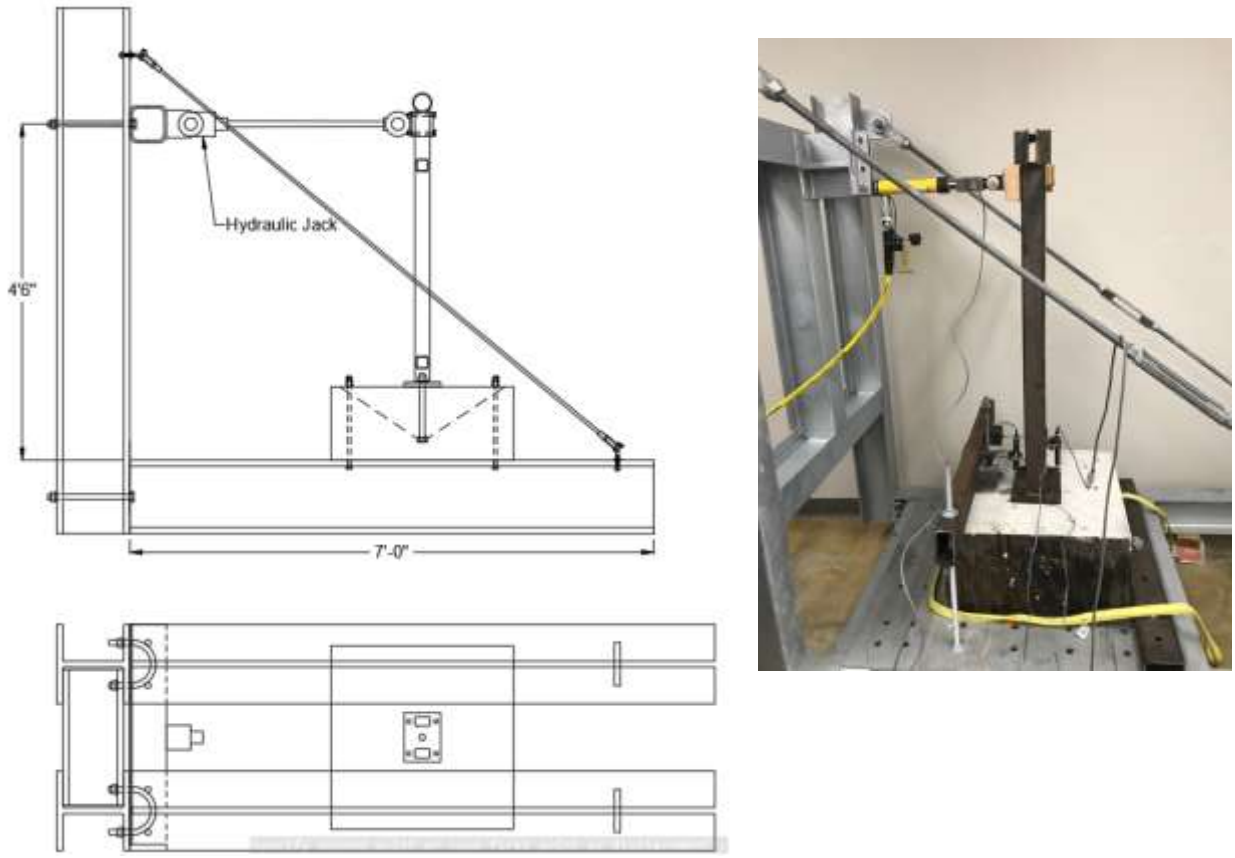

Figure 15 – Schemes 1 and 3 test setups

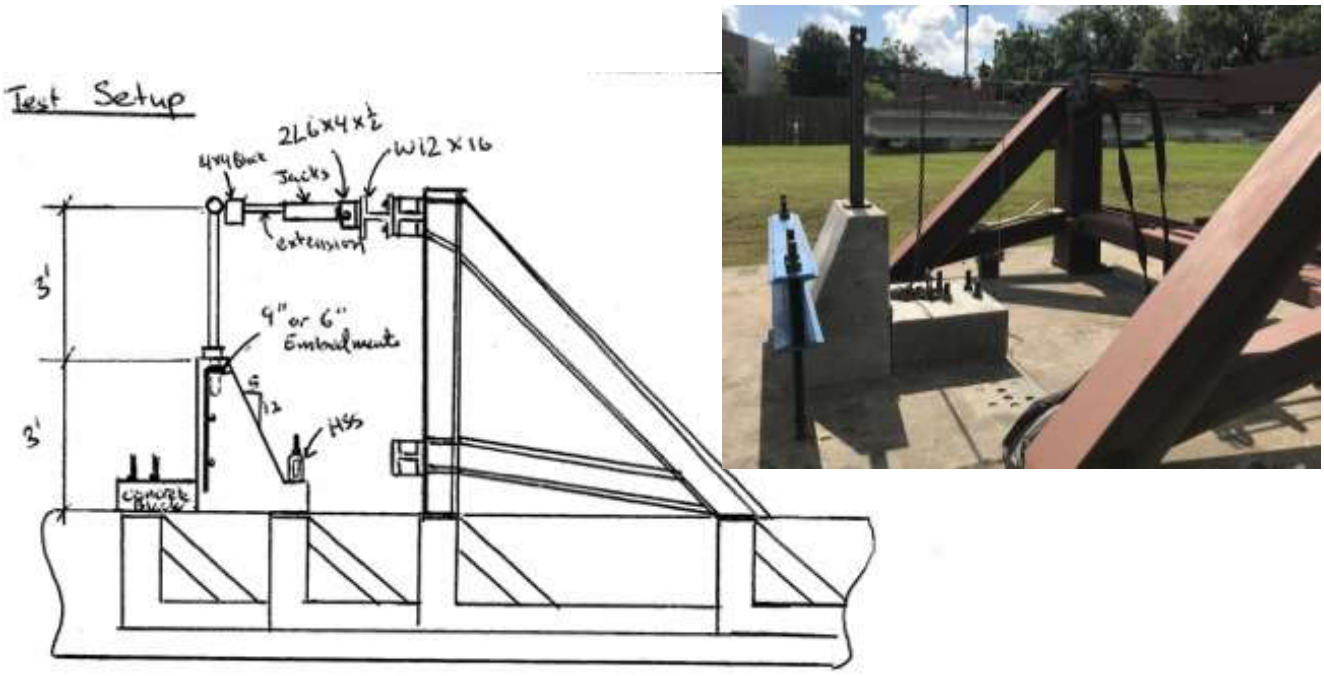

Figure 16: Gravity Wall Testing Setup

3.4 MATERIALS PROPERTIES AND SPECIFICATIONS

Concrete Material: Class NS concrete was obtained from two ready-mix concrete producers, Titan America and Argos in Melbourne and Tallahassee, respectively. The Titan America ready-mix concrete had an average compressive strength of 3,258 psi and was used for constructing the concrete blocks for the testing in Schemes 1 and 3. Argos ready-mix concrete had an average compressive strength of 3,711 psi and was used for the construction of the 3 ft gravity wall for the testing in Scheme 2.

Pedestrian Railing: The pedestrian railing was fabricated by Mahoney Supply, LLC in accordance with FDOT Design Standards, Index 852 (now Standard Plans Index 515-052). The pedestrian railing consisted of a 42 inches built-up section of two HSS $2^1/_2 \times 1^1/_2 \times {}^1/_8$ rectangular tubes that were connected at the top with an NSP $2^1/_2$ inches (Sch. 10) pipe and the bottom using an $8 \times 6 \times {}^5/_8$-inch steel plate.

Adhesive: Simpson Strong Tie ET-HP epoxy adhesive was used with a characteristic bond strength, $\tau_{k,uncr}$, of 940 psi for ${}^7/_8$ inches threaded rod. This adhesive was chosen because it represented the lowest possible characteristic bond strength among the adhesives that are listed on the FDOT Approved Products with an ICC-ES certification. It should be noted that other FDOT approved adhesives without ICC-ES certification only provide the average bond strengths that are much higher than the characteristic bond strength listed in the ICC-ES certification.

Anchor Bolt: The anchor bolt consisted of ${}^7/_8$ inches threaded rod, flat washer and hex nut that were all made with galvanized steel conforming to ASTM F1554 Grade 55, ASTM F436 and ASTM A194.

Bearing Pad: The bearing pad consisted of a ${}^1/_8$ inches thick neoprene pad with a durometer hardness of 60.

3.5 CONCRETE SPECIMENS FABRICATION

Concrete Block: A total of 27 concrete blocks were fabricated using ready-mix concrete and wood forms. There was no steel reinforcement inside the concrete blocks. Figure 17 illustrates the concrete block dimensions.

Gravity Wall: A total of 6 gravity walls were fabricated at the FDOT Structure Research Center. All gravity walls were 3 feet tall and 3 feet long. The top width was 8 inches and the bottom width was 2 feet-3 inches. Four gravity walls had two No. 4 vertical bars spaced at 1-foot-6-inches center-to-center, while two gravity walls had four No, 4 vertical bars spaced at 1-foot center-to-center. Figure 18 illustrates the reinforcement detail of the two gravity wall types.

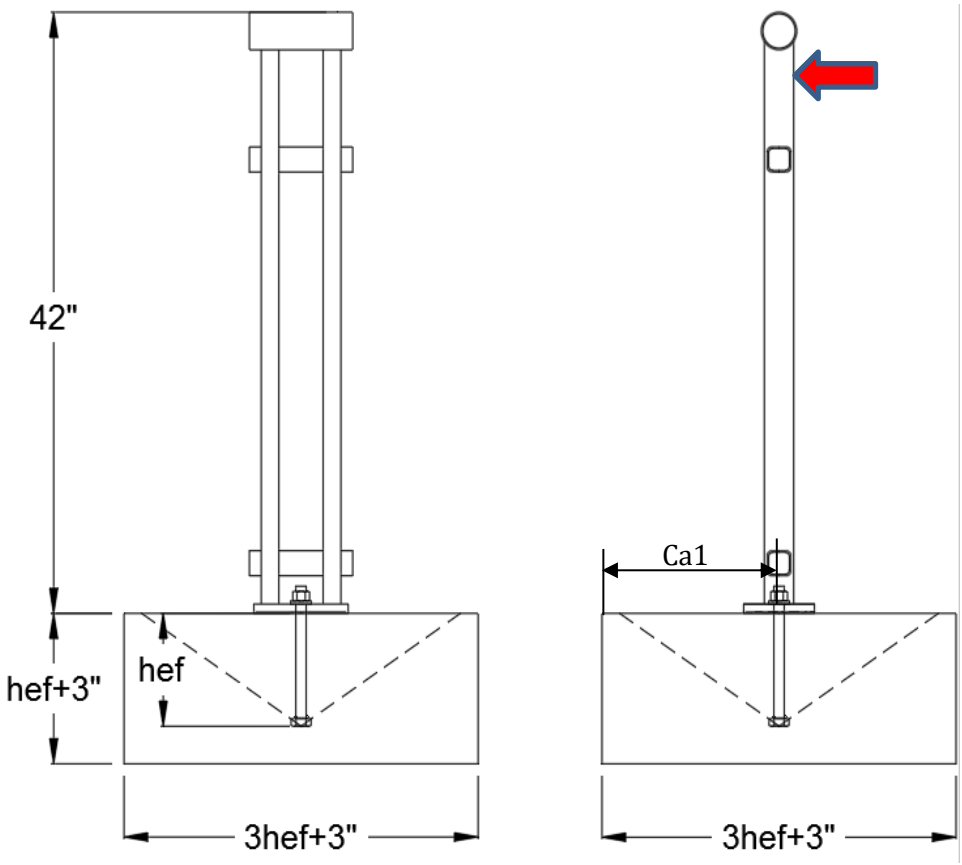

Figure 17: Concrete block dimensions

Adhesive Anchor Installation: The adhesive anchors were installed approximately 28 days after casting the concrete specimens in accordance with the manufacturer's installation instructions. First, a 1-inch hole was drilled to a specified depth using a rotary hammer drill. The dust from the hole was removed using a combination of oil-free compressed air at a pressure of 80 psi and a 1-$^{1}/_{8}$ inch nylon brush. Once the hole was free of dust, it was filled with the adhesive to approximately $^{2}/_{3}$ full followed by the anchor rod. The anchor rod was left undisturbed until the adhesive was fully cured (this depends on the ambient condition which is specified in the manufacturer's data sheet).

Pedestrian Railing Installation: The pedestrian railing was installed on the day of testing. A $^{1}/_{8}$ inches thick neoprene pad was placed in between the pedestrian railing base plate and concrete specimen. The hex nut was hand tightened using a wrench.

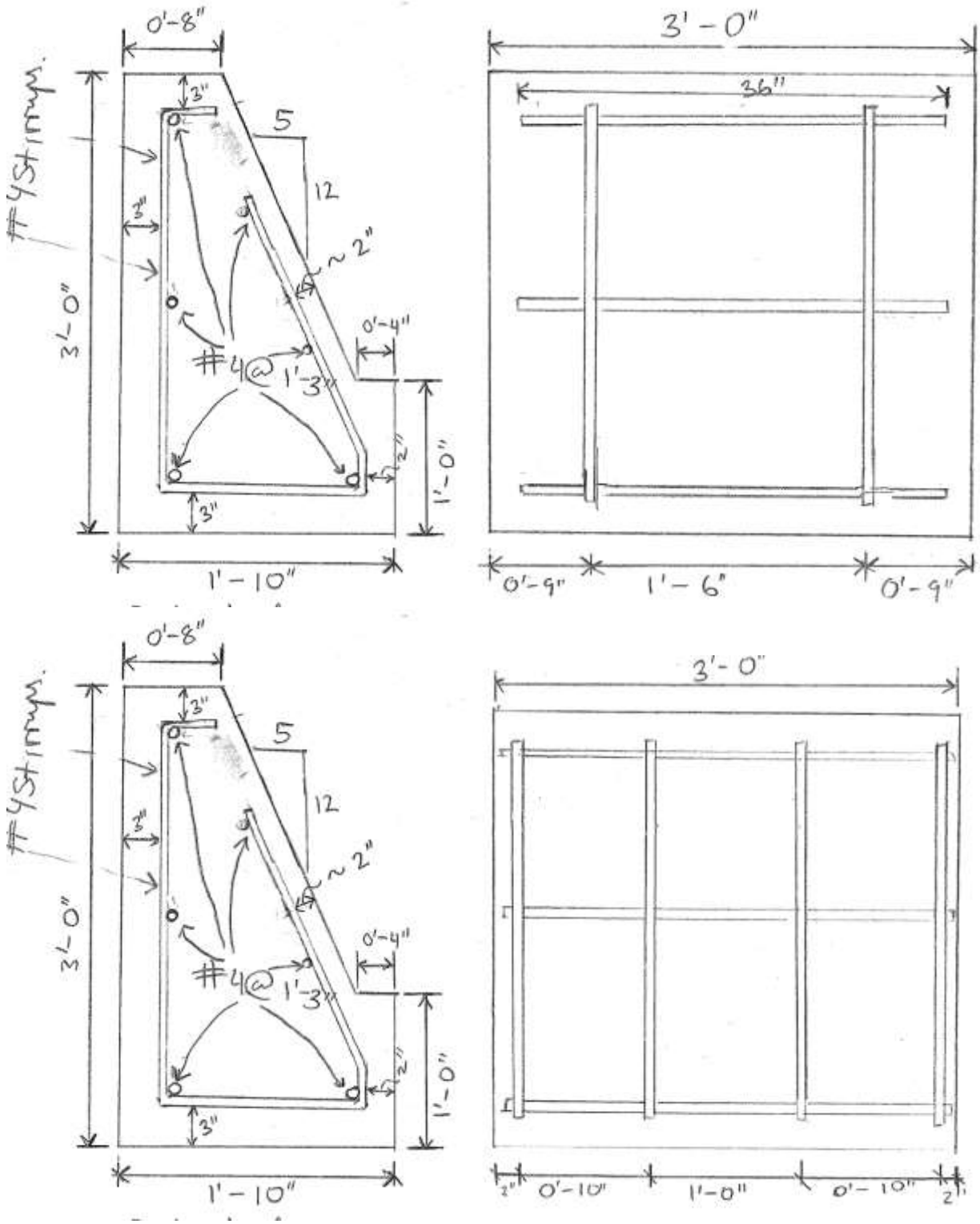

Figure 18: Drawing of the Gravity Wall

4. CHAPTER FOUR – EXPERIMENTAL RESULTS

4.1 SCHEMES 1 TEST RESULTS

Schemes 1 test was used to evaluate the confinement effect of metal railing narrow baseplates without the influence of edge distance. Table 3 provides a summary of the test results and corresponding calculations of adhesive breakout resistance using SDG and ACI procedures. It should be noted that the calculated values represented the nominal strengths rather than the design strength (i.e., load factor was not used). Furthermore, the confinement modification factor, Ψ_m was also not applied. As expected, the nominal tensile strength of the anchor bolt did not control the design but rather the nominal adhesive bond strength for both SDG and ACI procedures. However, no samples had an adhesive bond failure but rather a pry-out failure with concrete tension and shear cracks visibly observed on all tested samples, as illustrated in Figure 19.

When comparing the experimental breakout capacity to the nominal strengths using ACI and SDG procedures, the nominal concrete breakout strength using the ACI procedure closely matched the experimental results with an average percentage difference of 31.3%. The bond strength equations yielded higher average percentage differences of 72.8% and 56.8% using ACI and SDG procedures, respectively. Thus, it is recommended that the nominal concrete breakout strength be used in analyzing adhesive anchor breakout resistance for metal railings with narrow baseplates, considering that there is no standard for pry-out failure mode.

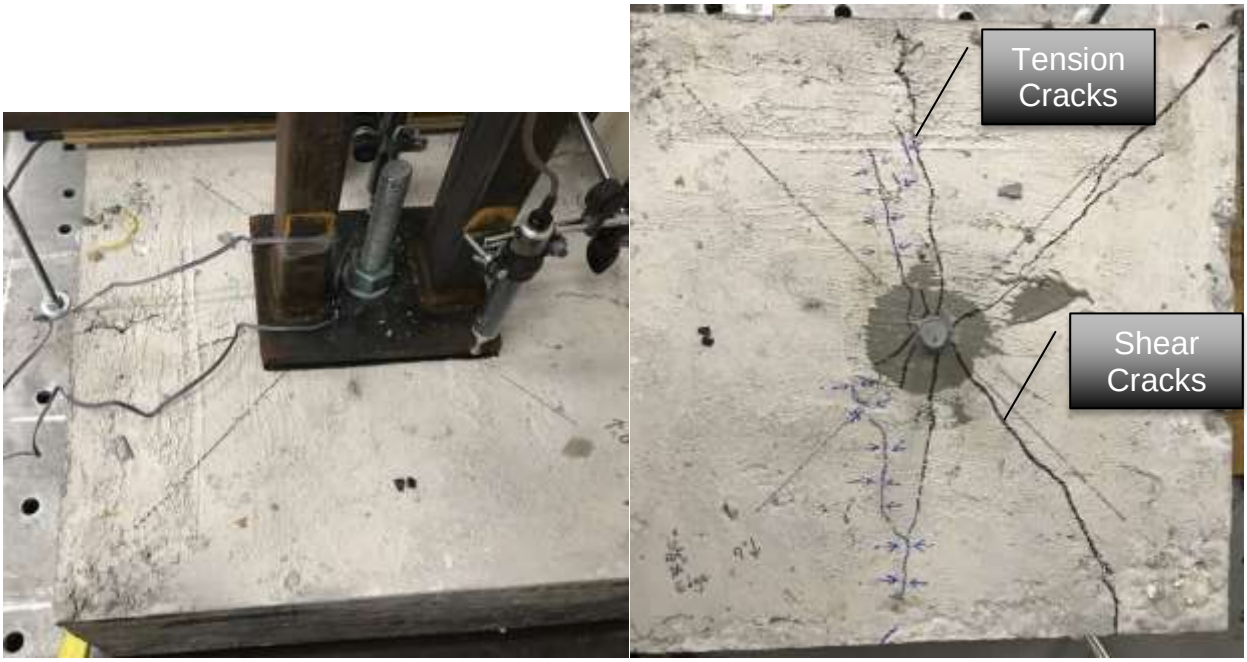

Figure 19: Typical Concrete Breakout/Pry-Out Failures Found in Concrete Block Specimens

Table 3: Test Results of Schemes 1 and 2

	Scheme 1			Scheme 2		
No.	S9	S6	S4	W12	W9	W9-X*
Embedment, h_{ef} (in)	9.00	6.00	4.00	12.00	9.00	9.00
Edge Distance, C_{a1} (in)	15.00	10.50	7.50	4.00	4.00	4.00
Loading Point, L (in)	37.50	37.50	37.50	32.50	32.50	32.50
Concrete Strength (psi)	3258			3711		
Experimental Test Results (lbs)	39525	23295	14096	40950	37700	33800
	42525	24750	15734	40300	40430	36400
	36405	21750	16866			
Average (lbs)	**39485**	**23265**	**15566**	**40625**	**39065**	**35100**
SDG Procedure (lbs)						
Tensile Strength, N_s	27059	27059	27059	27059	27059	27059
Adhesive Bond, N_o	23256	15504	10336	21231	15923	15923
ACI Procedure (lbs)						
Tensile Strength, N_{sa}	34630	34630	34630	34630	34630	34630
Adhesive Bond, N_a	19459	14396	10110	13583	13583	13583
Concrete Breakout, N_{cb}	30948	18695	10959	28476	20185	20185

*Specimens with four vertical rebars

4.2 SCHEME 2 TEST RESULTS

Scheme 2 test was used for evaluating the performance of adhesive anchor embedded in the gravity wall. The results of Scheme 2 are also summarized in Table 3. Overall, the primary failure mode in these specimens was the concrete breakout, which also matched well with the nominal concrete breakout resistance using the ACI procedure. There was only a slight increase of 3.99% in capacity between the specimens with 12-inch and 9-inch anchor bolt embedment length. This could be attributed to the shifting in failure mode from the concrete breakout to the adhesive bond failure found in gravity wall with 12-inch adhesive anchor embedment as illustrated in Figure 20.

Surprisingly, specimens with the two additional vertical rebars (W9-X) did not perform as well as the specimens with standard vertical rebars (W9). The reason for this could be attributed to the fact that the additional rebars forced the concrete breakout cone to be isolated between the two additional rebars spaced 1 foot apart opposed to the 1 foot-6 inch spacing used in standard reinforcement configuration. As a result, the W9-X samples ended up with a smaller breakout area and a reduction in breakout capacity. Figure 21 illustrates this in the top and bottom left photos showing narrower breakout cone confined within the 1-foot spacing as opposed to a much larger breakout cone observed in gravity wall with standard reinforcement configuration as displayed on the top and bottom right of Figure 21.

Figure 20: Adhesive Bond Failure in Gravity Wall with12-inch Adhesive Anchor Embedment

However, unlike the concrete block tested in Scheme 1, the nominal concrete breakout strengths are extremely conservative, with an average percentage difference of 70.0%. It should also be noted that this percentage difference does not include the strength reduction factor, $\phi = 0.75$, which would further increase the average percentage difference to 93.3%. It is suspected that the addition of steel reinforcement in the gravity wall helped prevent concrete from splitting, and therefore, increased the breakout capacity in the gravity wall to be much higher than the concrete block without reinforcement.

Another important note is how conservative the ACI procedure is when computing the nominal adhesive bond strength that governs the design criteria. In fact, if the ACI procedure is used, it would make it impossible to use a single adhesive anchor in gravity wall as the embedment length would no longer impact the design capacity. Although this was also observed in the experiment, the average percentage difference between the experimental test result and nominal adhesive bond using the ACI procedure was 182%. Therefore, it is recommended that the nominal adhesive bond strength not be used in determining the breakout resistance of adhesive anchor with the confinement effect.

Figure 21: Typical Concrete Breakout Failure Found in Gravity Wall Specimens

4.3 SCHEME 3 TEST RESULTS

Scheme 3 test was used to evaluate the impact of edge distance on adhesive breakout capacity. Table 4 summarizes the test results along with the nominal adhesive anchor breakout resistances using SDG and ACI procedures. Similar to the block concrete testing in scheme 1, the mode of failure was a splitting failure mode, as illustrated in Figure 22. The splitting is more severe with smaller edge distances. It is suspected that if additional reinforcement is provided to control splitting the breakout capacity would be much larger, similar to the gravity wall specimens. It should be noted that the ACI procedure does address the splitting failure mode using a modification factor, Ψ_{cp}. However, it seems that the computation of Ψ_{cp} is very conservative resulting in more significant reduction in nominal resistance as compared to experimental results. As a result, the nominal breakout resistance using ACI is slightly more conservative than the nominal adhesive bond resistance using SDG procedure.

Nevertheless, considering the observed failure mode is the concrete breakout, the nominal concrete breakout resistance using ACI procedure will still be used as the baseline for the analysis and should be recommended for determining the design strength.

Table 4: Scheme 3 Test Results

	Scheme 3					
Sample	S9-6	S9-4.5	S9-3	S6-6	S6-4.5	S6-3
Embedment, h_{ef} (in)	9.00	9.00	9.00	6.00	6.00	6.00
Edge Distance, C_{a1} (in)	6.00	4.50	3.00	6.00	4.50	3.00
Loading Point, L (in)	37.50	37.50	37.50	37.50	37.50	37.50
Concrete Strength (psi)	3258					
Experimental Test Results (lbs)	29579	24032	21740	21879	20949	13500
	27705	26431	25320	18155	21870	14580
	26895	24756	19760	24867	18450	12750
Average	**28060**	**25073**	**22273**	**21634**	**20423**	**13610**
SDG Procedure						
Tensile Strength, N_s	27059	27059	27059	27059	27059	27059
Adhesive Bond, N_o	20669	17056	13764	13779	11371	9176
ACI Procedure						
Tensile Strength, N_{sa}	34630	34630	34630	34630	34630	34630
Adhesive Bond, N_a	9680	9096	8513	10231	9614	8997
Concrete Breakout, N_{cb}	16764	14855	13050	12018	10216	8546

4.4 IMPACT OF SHORTER EMBEDMENT LENGTH

According to AASHTO LRFD, pedestrian railings are subjected to a design live load, *w* = 0.0050 klf. In addition, each longitudinal element (post) is also subjected to a concentrated load of 0.2 kips. For a post spacing of 8 feet, the ultimate lateral load can be calculated as follows:

P_{LL} = 0.20+0.050(8) = 0.60 kips
P_u = 1.75(0.60) = 1.05 kips (SDG procedure)
or
P_u = 1.6(0.60) = 0.96 kips (ACI procedure)

To determine the corresponding tension force on the adhesive anchor, the ultimate lateral load is multiplied by a moment arm, *L*, of 41 inches for a 42-inch pedestrian rail and divided by the distance between the adhesive anchor and reaction on the base plate of 2.5 inches. Assuming a strength reduction factor of 0.85 for SDG procedure and 0.75 for the ACI procedure, the required nominal resistance is:

$$\text{required } N_n = \frac{P_u}{\phi} \times \frac{L}{z} = \frac{1.05}{0.85} \times \frac{41}{2.5} = 20.26 \text{ kip} \quad \text{(SDG procedure)}$$

$$\text{required } N_n = \frac{P_u}{\phi} \times \frac{L}{z} = \frac{0.96}{0.75} \times \frac{41}{2.5} = 20.99 \text{ kip} \quad \text{(ACI procedure)}$$

Comparing these two required nominal strengths to experimental results summarized in Tables 3 and 4, it could be deduced that a reduced embedment length of 6 inches could be used in sidewalk provided that edge distance is at least 4.5 inches. Furthermore, the embedment length in gravity wall could be reduced to 9 inches. Further reduction in embedment length in gravity wall may be possible considering that there are reinforcements in the gravity wall to control splitting of the concrete. When comparing the results of W9 to S9-4.5, W9 has much higher resistance with a percentage difference of 55.9%.

Figure 22: Failure Modes of Adhesive Anchor with 6-, 4.5-, and 3-inch Edge Distance.

5. CHAPTER FIVE – DEVELOPMENT OF NEW DESIGN STANDARD FOR METAL RAILINGS

5.1 CONFINEMENT MODIFICATION FACTOR, Ψ_m

In order to develop a design procedure for FDOT to account for the confinement effect on adhesive anchor breakout resistance, several confinement modification factor equations were evaluated with the experimental results and other results from other literature. To do this, the confinement modification factor was computed from experimental results by taking the average breakout capacity divided by the nominal concrete breakout resistance obtained from the ACI procedure, i.e., $\Psi_m = \frac{N_{exp}}{N_{cb}}$. Table 5 summarizes the confinement modification factor equations from the literature.

Table 5: Confinement Modification Factor Equations

No.	Equation		References
1	$\Psi_m = \frac{1.5h_{ef}}{z}$	for $0 \leq \frac{z}{h_{ef}} \leq 1.5$	Zhao (1993)
	$\Psi_m = 1$	for $\frac{z}{h_{ef}} > 1.5$	
2	$\Psi_m = 2 - \frac{z}{h_{ef}}$	for $0 \leq \frac{z}{h_{ef}} \leq 1.0$	Bruckner (2001)
	$\Psi_m = 1$	for $\frac{z}{h_{ef}} > 1.0$	
3	$\Psi_m = \frac{2.5}{1+\frac{z}{h_{ef}}}$	for $0 \leq \frac{z}{h_{ef}} \leq 1.5$	Fichtner (2011) Parabolic Equations Adopted in SDG
	$\Psi_m = 1$	for $\frac{z}{h_{ef}} > 1.5$	
4	$\Psi_m = 2 - \frac{2z}{3h_{ef}}$	for $0 \leq \frac{z}{h_{ef}} \leq 1.5$	Fichtner (2011) Linear Equations
	$\Psi_m = 1$	for $\frac{z}{h_{ef}} > 1.5$	
5	$\Psi_m = 2.5 - \frac{z}{h_{ef}}$	for $0 \leq \frac{z}{h_{ef}} \leq 1.5$	Herzog (2015)
	$\Psi_m = 1$	for $\frac{z}{h_{ef}} > 1.5$	

The experimental results along with other data and equations are plotted in Figure 23. It is observed that out of the 5 equations, the Fichtner (2011) linear equation seems to provide the best approximation of the confinement effect on the adhesive anchor breakout resistance. However, the equation seems to provide an upper bound that may work well when the edge distance plays a role, which would be the case for FDOT

pedestrian railing. Nevertheless, a slightly more conservative linear equation is proposed as follow:

$$\Psi_m = 1.75 - \frac{z}{2h_{ef}} \quad \text{for } 0 \leq \frac{z}{h_{ef}} \leq 1.5 \qquad \text{Eq. 14}$$

$$\Psi_m = 1 \quad \text{for } \frac{z}{h_{ef}} > 1.5 \qquad \text{Eq. 15}$$

It is recommended that FDOT adopt the proposed equations that should be applied to the concrete breakout resistance using the ACI procedure.

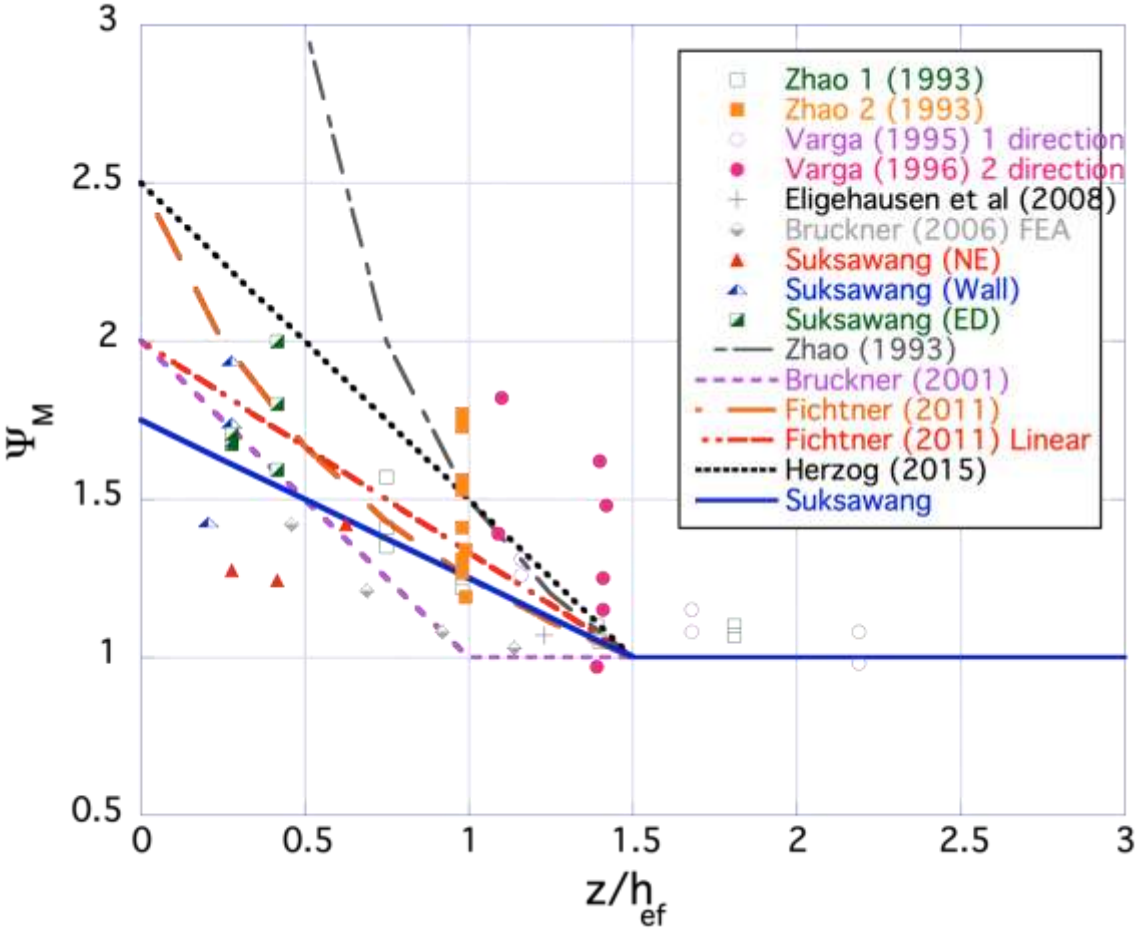

Figure 23: Factor Ψ_m as a function of z/h_{ef} ratio

5.2 PROPOSED DESIGN PROCEDURE

Based on the experimental results, the concrete cone breakout capacity from ACI318-14, Chapter 17 provides the most accurate model for predicting the adhesive anchor resistance. As a result, the ACI approach was used as a basis for developing the proposed design procedure.

5.2.1 Load Analysis

In many column-to-foundation connections including the connection for standard metal pedestrian/bicycle railings, the loading is not strictly tension but rather a moment couple of a tensile force in the adhesive anchor and a compressive force from the baseplates in the concrete breakout cone as shown in Figure 24, where the moment couple (M_u) and the ultimate tensile force (N_u) could be computed as follows,

$$M_u = P_u \times L_e \quad \text{Eq. 16}$$

$$N_u = C_u = \frac{M_u}{Z} \quad \text{Eq. 17}$$

$$P_u = \gamma_L(0.050S + 0.200) \quad \text{Eq. 18}$$

where, L_e is the distance between the center of the top rail to the concrete sidewalk (in); C_u is the compressive force acting on the concrete sidewalk that is caused by the moment couple (kips); Z is the center-to-center distance between N_u and C_u (in); and S is the center-to-center spacing of the post (ft). γ_L is the load factor for live load and can be taken as 1.60 in accordance with ACI. A γ_L of 1.75 could also be used but it should be noted that it would be overly conservative if the γ_L of 1.75 is used with ACI strength reduction factor (ϕ-factor).

The distance Z could be approximate for narrow baseplate with a single adhesive anchor in the center, as:

$$Z = {}^{5}/_{12}\, w \quad \text{Eq. 19}$$

where, w is the width of the baseplate. Z can also be taken as the center-to-center distance of two anchors that are perpendicular to the loading direction for narrow baseplate with four adhesive anchors.

5.2.2 Design Methodology

To design, ACI provides three main limit states: (1) steel strength in tension, (2) concrete breakout strength in tension, and (3) bond strength of adhesive anchor in tension for post-installed adhesive anchors. However, based on experimental results, only the first two limit states are proposed for designing adhesive anchors on a pedestrian railing with a narrow metal baseplate. Additionally, a new confinement medication factor is also proposed.

Steel Strength in Tension

The limit state of steel strength in tension is:

$$\phi N_{sa} \geq N_u \quad \text{Eq. 20}$$

The design tensile strength for the adhesive anchor steel is given as:

$$\phi N_{sa} = \phi_{sa} A_{se} f_{uta} \qquad \text{Eq. 21}$$

where ϕ_{sa} is the strength reduction factor and can be taken as 0.75. f_{uta} is the anchor steel ultimate strength and should be limited to 1.9 times the yield strength or 125 ksi. For threaded rods and headed bolt anchors, the effective anchor area can be computed using ASME B1.1 as:

$$A_{se} = \frac{\pi}{4}\left(d_a - \frac{0.9743}{n_t}\right)^2 \qquad \text{Eq. 22}$$

where, d_a and n_t are the diameter and number of threads per inch of the anchor rod, respectively.

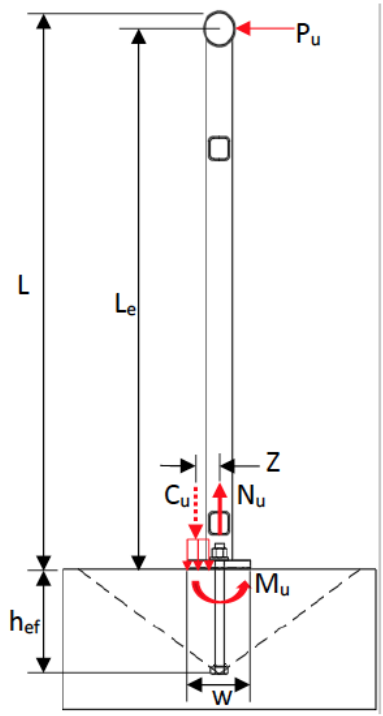

Figure 24—Effect of moment on standard metal pedestrian/bicycle railings connections as adopted from Eligehausen et al (2014)

Concrete Breakout Strength

The limit state of concrete breakout strength in tension is:

$$\phi N_{cb} \geq N_u \qquad \text{Eq. 23}$$

The design concrete breakout strength in tension is given as:

$$\phi N_{cb} = \phi_{cb} \frac{A_{Nc}}{A_{Nco}} \Psi_{ed} \Psi_{cp} \Psi_m N_b \quad \text{Eq. 24}$$

and

$$N_b = k_c \lambda_a \sqrt{f_c'} h_{ef}^{1.5} \quad \text{Eq. 25}$$

where ϕ_{cb} is the strength reduction factor and can be taken as 0.65; k_c is the coefficient for basic concrete breakout strength in tension that can be taken as 24[1]. λ_a is the modification factor to reflect the reduced mechanical properties of lightweight concrete in certain anchorage application. For pedestrian railing, this factor can be taken as 1 since normal weight concrete is used. f_c' is the specified 28-day compressive strength of concrete and h_{ef} is the embedment length.

A_{Nco} is the projected concrete failure area of a single anchor with an edge distance equal to or greater than $1.5h_{ef}$ and can be taken as:

$$A_{Nco} = 9h_{ef}^2 \quad \text{Eq. 26}$$

A_{Nc} is the actual projected concrete failure area that is approximated as the base of the rectilinear geometrical figure that results from projecting the failure surface outward $1.5h_{ef}$ from the centerline of the anchor as illustrated in figure 25.

Additionally, for anchor loaded in tension and spaced closer than $1.5h_{ef}$, a reduction factor for edge effects, Ψ_{ed}, given by Equation 27 must be applied. For anchor spacing equal and greater than $1.5h_{ef}$, Ψ_{ed} is taken as 1.

$$\Psi_{ed} = 0.7 + 0.3 \frac{c_{a,min}}{1.5h_{ef}} \quad \text{Eq. 27}$$

where, $c_{a,min}$ is the minimum edge distance.

[1] It should be noted that ACI recommends $k_c = 17$. However, this value is multiplied with a modification factor, Ψ_c, that is omitted from Equation 24. This factor can be taken as 1.4 for uncracked concrete under service load resulting in the factors to be $\Psi_c k_c = 24$.

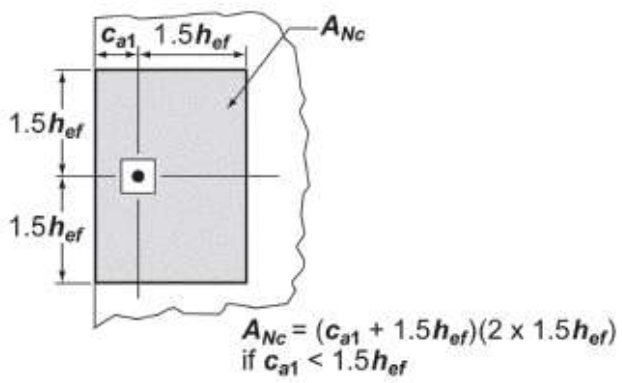

Figure 25—Examples of concrete breakout failure projected area for a single anchor (ACI 318, 2014)

For plain concrete (e.g. concrete sidewalk) without supplementary reinforcement to control splitting failure in the concrete, a modification factor, Ψ_{cp} was introduced in ACI and can be computed as:

If $c_{a,min} \geq c_{ac}$, then $\Psi_{cp} = 1.0$ Eq. 30

If $c_{a,min} < c_{ac}$, then $\Psi_{cp} = \frac{c_{a,min}}{c_{ac}}$ Eq. 31

but Ψ_{cp} cannot be taken less than $1.5h_{ef}/c_{ac}$, where c_{ac} is the critical edge distance that can be taken as $2h_{ef}$ or the recommended value from ICC-ES evaluation report of the adhesive. If $2h_{ef}$ is used, then $\Psi_{cp} = 0.75$, which seems to be overly conservative considering that this factor was developed for expansion and undercut anchors. In fact, the NCHRP Report 757 on Long-Term Performance of Epoxy Adhesive Anchor System by Cook, Douglas, Davis, and Liu (2013) do not recommend the use of this factor at all, which seems to agree to the testing result performed in this study. Therefore, it is recommended that $\Psi_{cp} = 1.0$ should be used in lieu of Equations 30 and 31.

For anchors loaded in tension with the metal baseplate provide confinement effect, the modification factor, Ψ_m given in Equations 14 and 15 can also be used.

5.3 DESIGN EXAMPLES

5.3.1 Unreinforced Concrete Sidewalk

Given:
$^7/_8$ in ASTM F1554 Grade 55 threaded rod with 9 tread/in

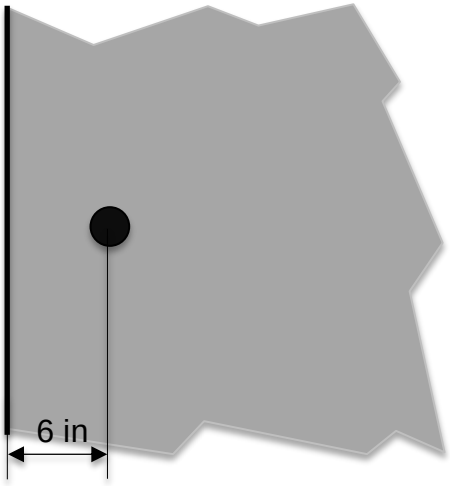

$$A_{se} = \frac{\pi}{4}\left(\frac{7}{8} - \frac{0.9743}{9}\right)^2 = 0.462 \text{ in}^2$$

$$F_{uta} = 75 \text{ ksi}$$

Embedment Length of 6 in.
$h_{ef} = 6$ in

For a 6 × 8 in base plate
$$z = \frac{5}{12} \times 6 = 2.5 \text{ in}$$

Anchor is located 6 in from nearest edge
$c_{a,min} = 6$ in

Class I Concrete with a design strength of 4,000 psi[2]
$f_c' = 4{,}000$ psi

42 in pedestrian rail post with $2^1/_2$" NPS top rail and $^1/_8$" neoprene pad

$$L_e = 42 + \frac{1}{8} - \frac{2.875}{2} = 40.69 \approx 41 \text{ in}$$

Design Loads:
Determine the horizontal load acting on the post of the pedestrian railing assuming a center-to-center spacing of 8 ft.

$$P_u = 1.6 \times (0.050 \times 8 + 0.2) = 0.96 \text{ kips}$$

Determine the tensile load on the anchor from the moment of a couple.

$$M_u = 0.96 \times 41 = 39.36 \text{ kip-in}$$

[2] Although FDOT specifies the minimum 28-day strength of Class I concrete to be 3,000 psi, it needs to be increased to 4,000 psi in this example to ensure that an embedment length of 6 can be used. It should be noted that if 3,000 psi concrete is used, the embedment would have to be increased to 7 in. Considering that there is no significant cost difference for higher strength concrete, it was decided that higher strength concrete be used.

$$N_u = \frac{39.36}{2.5} = 15.74 \text{ kips}$$

Steel Strength in Tension:

Comparing the design strength due to anchor tension failure with the design load.

$$\phi N_{sa} = 0.75 \times 0.462 \times 75 = 26.0 \text{ kips} > 15.74 \text{ kips [OK]}$$

Concrete Breakout Strength:

Calculate the nominal resistance due to concrete breakout failure

$$N_b = \frac{1}{1000} 24 \times 1 \times \sqrt{4{,}000} \times 6^{1.5} = 22.31 \text{ kips}$$

Determine the projected influence area with and without the influence of edge effects.

$$A_{Nc} = (6 + 1.5 \times 6)(2 \times 1.5 \times 6) = 270 \text{ in}^2$$

$$A_{Nco} = 9 \times 6^2 = 324 \text{ in}^2$$

Calculate the modification factor for edge effects

Since $c_{a,min} < 1.5h_{ef}$

$$\Psi_{ed} = 0.7 + 0.3\frac{6}{1.5 \times 6} = 0.90$$

Assume there is no splitting effects

$$\Psi_{cp} = 1.0$$

Calculate the modification factor for confinement effects

$$\Psi_m = 1.75 - \frac{2.5}{2 \times 6} = 1.54$$

Comparing the design resistance due to concrete breakout failure with the design load.

$$\phi N_{cb} = 0.65 \times \frac{270}{324} \times 0.90 \times 1.0 \times 1.54 \times 22.31 = 16.75 \text{ kips} > 15.74 \text{ [OK]}$$

5.3.2 Reinforced Concrete Gravity Wall

Given:
$^7/_8$ in ASTM F1554 Grade 55 threaded rod with
9 tread/in

$$A_{se} = \frac{\pi}{4}\left(\frac{7}{8} - \frac{0.9743}{9}\right)^2 = 0.462 \text{ in}^2$$

$$F_{uta} = 75 \text{ ksi}$$

Embedment Length of 8 in.
$h_{ef} = 8$ in

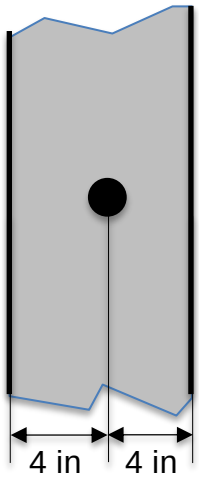

For a 6 × 8 in base plate
$$z = \frac{5}{12} \times 6 = 2.5 \text{ in}$$

Anchor is located 4 in from nearest edge
$c_{a,min} = 4$ in

Class I Concrete with a design strength of 3,000 psi
$f_c' = 3{,}000$ psi

42 in pedestrian rail post with $2^1/_2$" NPS top rail and $^1/_8$" neoprene pad

$$L_e = 42 + \frac{1}{8} - \frac{2.875}{2} = 40.69 \approx 41 \text{ in}$$

Design Loads:
Determine the horizontal load acting on the post of the pedestrian railing assuming a center-to-center spacing of 8 ft.

$$P_u = 1.6 \times (0.050 \times 8 + 0.2) = 0.96 \text{ kips}$$

Determine the tensile load on the anchor from the moment of a couple.

$$M_u = 0.96 \times 41 = 39.36 \text{ kip-in}$$

$$N_u = \frac{39.36}{2.5} = 15.74 \text{ kips}$$

Steel Strength in Tension:
Comparing the design strength due to anchor tension failure with the design load.

$$\phi N_{sa} = 0.75 \times 0.462 \times 75 = 26.0 \text{ kips} > 15.74 \text{ kips [OK]}$$

Concrete Breakout Strength:

Calculate the nominal resistance due to concrete breakout failure

$$N_b = \frac{1}{1000} 24 \times 1 \times \sqrt{3{,}000} \times 8^{1.5} = 29.74 \text{ kips}$$

Determine the projected influence area with and without the influence of edge effects. Although the influence area should be calculated using the top surface area of the gravity wall, a larger influence area is used based on experimental observation. The same influence area equation as the sidewalk, i.e., $A_{Nc} = \left(c_{a,min} + 1.5h_{ef}\right)\left(2 \times 1.5h_{ef}\right)$, is used here.

$$A_{Nc} = (4 + 1.5 \times 8)(2 \times 1.5 \times 8) = 384 \text{ in}^2$$
$$A_{Nco} = 9 \times 8^2 = 576 \text{in}^2$$

Calculate the modification factor for edge effects

Since $c_{a,min} < 1.5h_{ef}$

$$\Psi_{ed} = 0.7 + 0.3 \frac{4}{1.5 \times 8} = 0.80$$

Assume reinforcement controls splitting in concrete.

$$\Psi_{cp} = 1.0$$

Calculate the modification factor for confinement effects

$$\Psi_m = 1.75 - \frac{2.5}{2 \times 8} = 1.59$$

Comparing the design resistance due to concrete breakout failure with the design load.

$$\phi N_{cb} = 0.65 \times \frac{384}{576} \times 0.80 \times 1.0 \times 1.59 \times 29.74 = 16.39 \text{ kips} > 15.74 \text{ [OK]}$$

5.4 PROPOSED DESIGN STANDARD

The proposed design standard drawing of metal railing with adhesive anchor is provided in Appendix A. Figure 26 illustrates new sidewalk pavement details and Table 6 provides the proposed modification to the embedment length. It should be noted that this table is based on structural concrete (i.e., Class I Concrete) and not Class NS.

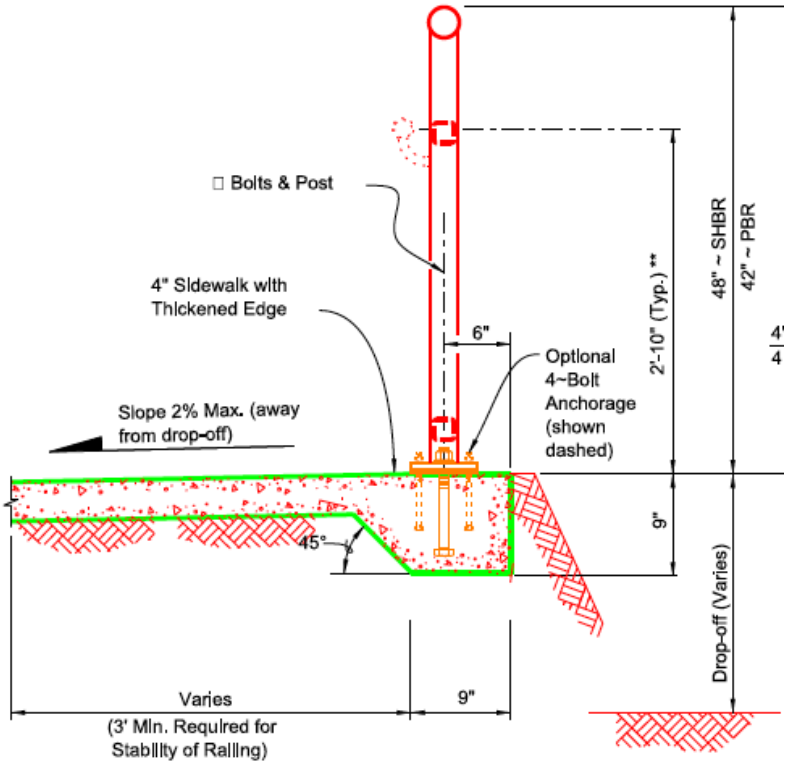

Figure 26-Modified Concrete Pavement Slab details

Table 6-Modified embedment length

ANCHOR BOLT TABLE							
CASE	STRUCTURAL TYPE	DIMENSIONS			ANCHOR LENGTH		
		A Edge Dist.	B Edge Dist.	C Embedment	C-I-P HEX Head Bolt	Adhesive Anchor	ANCHOR SIZE
I	Unreinforced Concrete	6"	1'-2"	6"	7 1/2"	8"	7/8" Ø
IIa	Reinforced Concrete	4"	4"	8"	9 1/2"	10"	7/8" Ø
IIb	Gravity Wall Index 400-011	4 1/2"	3 1/2" @ top	8"	9 1/2"	10"	7/8" Ø
III	Step Cheekwall	4 1/2"	4 1/2"	8"	9 1/2"	10"	7/8" Ø
IV	Varies	5"	5"	5"	6 1/2"	7"	7/16" Ø

6. CHAPTER SIX – OTHER APPLICATIONS

6.1 POTENTIAL EXPANDED USE

The proposed confinement modification factor can be used to all post-installed anchors as it is applied to the concrete breakout strength. It could also be applied to other failure modes, but more testing would be needed to confirm its applicability. Considering the increase in concrete breakout strength for other mechanical post-installed anchors, particularly a screw anchor. It is possible that with the proposed modification factor, these anchor systems could be used instead of an adhesive anchor for pedestrian railing. The current design concrete breakout strength of the screw anchor is approximately 9,800 – 15,000 lbs depending on concrete compressive strength so if modification factor of $\Psi_m = 1.5$ is applied, the design concrete breakout capacity could increase to 14,700 to 22,500 lbs, which meet the required strength of 15,600 lbs if higher concrete strength concrete is used. However, the design pullout strength would have to be evaluated to determine the governed failure mode.

Using post-installed mechanical anchors can further reduce the installation cost and time as there is no additional adhesive cost and no need to wait for the adhesive to harden, which takes between 24 – 72 hours depending on the ambient temperature.

6.2 PROPOSED TESTING PROCEDURE

To determine the failure mode and the applicability of the confinement modification factor, two testing schemes are proposed. The first scheme consists of nine unreinforced concrete blocks to evaluate various screw anchor embedment lengths, i.e., 9, 6, and 4 inches. All tests should be performed with 6-inch edge distance to evaluate the failure mechanism of the screw anchor and determine the critical embedment length which shifts the failure mode from concrete breakout failure to screw pullout failure. The same test setup is proposed using a reaction frame to push or pull the top rail of a single pedestrian rail post as illustrated in Figure 15.

The second testing scheme consists of testing nine 3-ft gravity wall sample at FDOT structure lab using the same setup as the one performed for adhesive anchors. Figure 16 illustrates the test setup used previously in this project. This testing scheme provides the smallest edge distance, as well as failure mechanism, different than the one in unreinforced concrete block. The reinforcement in the gravity wall provides additional strength from concrete side-face blowout and splitting. The shape and reinforcement of the gravity wall also provided a much larger critical concrete breakout area beyond the surface area at the top of the gravity wall. As observed in Figure 21, the concrete breakout cone extended at least 6 inches below the top surface; and because of the gravity shape there is an increase in the surface area. Due to the limitation of the length of the screw anchor, the same embedment length, i.e., 9, 6, and 4 inches will also be evaluated. Table 7 provides a summary of a list of parameters and sample size of the two testing schemes.

Table 7: List of experimental parameters

	Scheme 1			Scheme 2		
ID	UR-9	UR-6	UR-4	RGW-9	RGW-6	RGW-4
Sample Size	30×20×12-in			3×3×2.25 ft		
Embedment (in)	9	6	4	9	6	4
z/h_{ef}	0.28	0.42	0.63	0.28	0.42	0.63
Edge Distance (in)	6.0	6.0	6.0	4.0	4.0	4.0
No. of Specimens	3	3	3	3	3	3

7. CHAPTER SEVEN – RECOMMENDATION AND CONCLUSIONS

The following conclusions and recommendations are made:

1. The failure mode of adhesive anchors installed in pedestrian railing with narrow baseplates closely matched the concrete breakout failure mode, and therefore, the concrete breakout failure resistance equation provided by ACI should be used when computing the adhesive anchor resistance.
2. Other than the gravity wall with 12-inch anchor embedment length, no adhesive failure was observed despite the fact that all equations using both SDG and ACI procedures predicted adhesive failure mode. This observation was made even with the use of the lowest strength adhesive that is FDOT approved. Thus, both equations are too conservative and should be omitted when evaluating adhesive anchor with confinement effect provided that the adhesive has an uncharacteristic strength of 940 psi or higher.
3. It is recommended that FDOT modifies the Design Standard, Index 852 & 862 (now Standard Plans Index 515-052 & 515-062) to allow for a reduced embedment length of 6 inches for sidewalk and 9 inches for gravity wall. This would provide significant cost saving and possibly improve quality as large embedment length is challenging and time-consuming to install in the field.
4. It is also recommended that FDOT adopts the proposed confinement modification factor, Ψ_m, that can be applied to either the current SDG adhesive bond resistance or ACI concrete breakout resistance to improve the accuracy of the design for adhesive anchor with confinement effect.
5. It is also recommended that FDOT develop a pool fund with AASHTO to investigate the validity of the concrete splitting modification factor, Ψ_{cp}, as this factor significantly reduces the concrete breakout and adhesive bond resistances by as much as 50% which does not seem to be supported by the limited test results in this study.
6. As the scope of this research project is limited to Simpson Strong Tie ET-HP epoxy adhesive, more research is needed to investigate other FDOT approved products that do not meet ICC-ES certification, i.e., products that met FDOT Method of Test

FM-5-568 considering that these products will not meet the new AASHTO specification.

7. Considering there could be further potential cost saving using screw anchor as well as the potential conflict with adhesive products not meeting ICC-ES certification, it is recommended that screw anchor as described in Chapter 6 be investigated.

8. REFERENCES

1. AASHTO (2016), “LRFD Bridge Design Specifications, Customary U.S. Unites,” 7th Edition, with 2015 and 2016 Interim Revisions.
2. ACI 318-14 (2014), “Building Code Requirements for Structural Concrete”
3. ACI 355.4 (2011) “Qualification of Post –Installed Adhesive Anchors in Concrete (ACI 355.4-11)”
4. ASME (2003) “Unified Inch Screw Threads (UN and UNR Thread Form)” (ASME B1.1-03)
5. Bruckner, M., Eligehausen, R. and Ozbolt, J. (2001) “Influence of bending compressive stresses on the concrete cone capacity,” Connection between Steel and Concrete, Eligehausen, R. (Editor), RILEM Publications
6. Cook, R. A. (1993) “Behavior of Chemically Bonded Anchors,” ASCE Journal of Structural Engineering, V. 119, No. 9, pp. 2744-2762.
7. Cook, R. A., Doerr, G. T., and Klingner, R. E. (1993) “Bond Stress Model for Design of Adhesive Anchors,” ACI Structural Journal, V. 90, No. 5, pp. 514-524.
8. Cook, R. A., Kunz, J., Fuchs, W., and Konz, R. C. (1998) “Behavior and Design of Single Adhesive Anchors under Tensile Load in Uncracked Concrete,” ACI Structural Journal, V. 95, No. 1, pp. 9-25.
9. Cook, R. A., Konz, R. C., and Richardson, D. S. (1996) “Specifications for Adhesive-Bonded Anchors and Dowels,” Final Report submitted to FDOT, No. FL/DOT/RMC/0662-9195, p. 140
10. Cook, R. A. and Beresheim S. D. (2002) “Post-Installed Adhesive-Bonded Splices in Bridge Decks,” Final Report submitted to FDOT, No. BC354 RPWO #2, p. 83
11. Davis, T. M. (2012) “Sustained Load Performance of Adhesive Anchor Systems in Concrete” Ph.D. Thesis, University of Florida, p. 571
12. Eligehausen, R., Mallée, R., Rehm, G. (1984) “Befestigungen mit Verbundankern,” Betonwerk + Fertigteil-Technik, No. 10, pp. 686-692, No. 11, pp. 781-785, No. 12, pp. 825-829 (in German).
13. Eligehausen, R., Appl, J. J., Lehr, B., Meszaros, J., and Fuchs, W. (2004) “Tragverhalten und Bemessung von Befestigungen mit Verbünddubeln unter Zugbeanspruchung, Teil 1: Einzeldübel mit großem Achsund Randabstand,” Beton und Stahbetonbau 99, No. 7, pp. 561-571.
14. Eligehausen, R., Appl, J. J., Lehr, B., Meszaros, J., and Fuchs, W (2005) “Tragverhalten und Bemessung von Befestigungen mit Verbünddubeln unter Zugbeanspruchung, Teil 2: Gruppen und Einzeldübel am Bauteilrand,” Beton und Stahbetonbau 100, No. 10, pp. 856-864.

15. Eligehausen, R., Cook, R. A., and Appl, J. (2006) “Behavior and Design of Adhesive Bonded Anchors” ACI Structural Journal, V. 103, No. 6, pp. 822-831
16. Eligehausen, R., Mallee, R., and Silva, J. F. (2006) Anchorage in Concrete Construction, Ernst & Sohn, Berlin, Germany, pp. 378
17. Eligehausen, R., Kuhlmann, U., Fichtner, S., Rybinski, M. (2008) “Modelierung biegeweicher Stützenfüße im Stahl- und Verbundbau als integriertes System von Tragwerk und Fundament,” Test Report, Institut für Wekstoffe im Bauwesen, Universität Stuttgart, not publish
18. Eligehausen, R., Mahrenholtz, C., Akguzel, U., and Pampanin, S. (2014) “Bridging the gap between design provisions for connections using anchorage or strut-and-tie models” ACI SP 296-5, pp. 5.1 – 5.16
19. FDOT (2000) “Anchor System Tests for Adhesive-Bonded Anchors and Dowels,” Method of Test FM-5-568, Retrieved from https://www.fdot.gov/materials/administration/resources/library/publications/fstm/bynumber.shtm
20. FDOT (FY2016-2017) “Steel Pedestrian/Bicycle Railing,” Design Standards, Index 852, p. 8
21. FDOT (2017) “FDOT Structures Manual,” Volume 1, Structures Design Guidelines.
22. FDOT (2019), “Bridge Pedestrian/Bicycles Railing (Steel)” Standard Plans Index 515-052, Retrieved from https://www.fdot.gov/design/standardplans/current/default.shtm
23. Fichtner, S (2011) “Untershchungen zum Tragverhalten von Gruppenbefestigungen unter Berücksichtigung der Ankerplattendicke und einer Mörtelshicht,” Ph.D Dissertation, Universität Stuttgart, p. 301
24. Fuchs, W., Eligehausen, R., Breen, J. E., (1995) “Concrete Capacity Design (CCD) Approach for Fastening to Concrete,” ACI Structural Journal, V. 92, No. 1, pp. 73-94.
25. Herzog, M. B. (2015) “Beitrag zur Vereinheitlichung der Bemessung im Stahlbetonbau und in der Befestigungstechnik” Ph.D Dissertation, Universität Stuttgart, p. 457
26. Kunz, J, Cook, R. A., Fuchs, W., Spieth, H. (1998) “Tragverhalten und Bemessung von chemichen Befestigungen” Beton- und Stahlbetonbau, 93, No. 1, pp. 15-19, No. 2, pp. 44-49 (in German)
27. Lehr, B. (2003) “Tragverhalten von Verbunddübeln unter zentrischer Belastung um ungerisenen Beton – Gruppenbefestigungen und Befestigungen am Bauteilrand,” Ph.D Dissertation, Universität Stuttgart (in German)
28. McVay, M., Cook, R. A., Krishnamurthy, K. (1996) “Pullout Simulation of Post installed Chemically Bonded Anchors” ASCE Journal of Structural Engineering, V. 122, No. 9, pp. 1016-1024
29. Meszaros, J. (1999) “Tragverhalten von Verbunddübeln im ungerissenen und gerissen Beton”, Doctor Thesis, Universität Stuttgart.
30. Varga, J. and Eligehausen, R. (1995) “Test Program for Fastentings with Headed Studs, Part 1,” Report No. Te 696/1 – 95/4, Institut für Wekstoffe im Bauwesen, Universität Stuttgart, not publish

31. Varga, J. and Eligehausen, R. (1996) “Test Program for Fastentings with Headed Studs, Part 2,” Report No. Te 696/03 – 96/05, Institut für Wekstoffe im Bauwesen, Universität Stuttgart, not publish
32. Zamora, N. A., Cook, R. A., Konz, R. C., Consolazio, G. R. (2003) “Behavior and Design of Single Headed and Unheaded Grouted Anchors under Tensile Load,” ACI Structural Journal, V. 100, No. 2, pp. 222-230
33. Zhao, G.C. (1993) “Tragverhalten von randfernen Kopfbolzenverankerungen bei Betonausbruch,” Ph.D. Dissertation, University of Stuttgart, 1993 (in German)